

Rheinische Friedrich-Wilhelms-Universität Bonn
Master Course, WS 2010/2011

Computational Physics Project



Title: **Fractal Growth**

Authors: **Anton Iakovlev & Martin Garbade**

Examiner: Prof. Carsten Urbach

Tutor: Simon Tölle

Date: March 17, 2011
Bonn

Contents

1	Introduction	3
2	Fractals	3
2.1	Basic Definitions and Notions	3
2.2	Measuring Fractal Dimension in Computer Simulation	7
2.3	DLA Model	8
3	Computer Simulation of Fractal Growth	8
3.1	Irreversible DLA Model of Single Immobile Cluster Formation	8
3.1.1	Simulation Method	8
3.1.2	Results for Two-Dimensional Clusters	10
3.1.3	Results for Three-Dimensional Clusters	16
3.2	Irreversible DLA Model of Multiple Mobile Clusters Formation	20
3.2.1	Simulation Method	20
3.2.2	Results	20
3.3	Adaptive Growth Model	25
3.3.1	Simulation Method	25
3.3.2	Results	26
4	Conclusions	31
5	Literature	33
A	Additional data from 2D DLA clusters simulation ($p_{nn} = 1$)	34
B	Additional data from 2D DLA clusters simulation ($p_{nn} < 1, p_{snn} = 0$)	36
C	Additional data from 2D DLA clusters simulation ($p_{nn} = 0, p_{snn} \neq 0$)	38
D	Additional data from 2D DLA clusters simulation ($p_{nn} \neq 0, p_{snn} \neq 0$)	39
E	Additional data from 3D DLA clusters simulation ($p_{nn} = 1$ and $p_{nn} = 0.25$)	41
F	Additional data from adaptive network simulation	44

1 Introduction

The rapid advancement of the computational power over the last years opens new perspectives for the study of many-particle systems. In the current report we present the investigation of the fractal growth by means of the Monte Carlo simulation. First, we study the diffusion limited agglomeration (DLA) model of the irreversible growth of a single cluster grown from a seed particle fixed in the center of the system in two- and three-dimensional space. Next, the DLA model of the irreversible growth for the multiple mobile clusters is examined. Then follows the simulation of the adaptive network growth based on the Eden model. The density-density correlation function and the radius of gyration along with the other relevant fractal quantities are calculated. The fractal dimensions are calculated in two ways, first, from the radius of gyration and, second, from the density-density correlation function. The dependency on the parameters of the model is investigated and discussed. The results are compared with the former works by Meakin ([7],[10],[12]).

2 Fractals

2.1 Basic Definitions and Notions

One of the most important characteristic features of fractals is self-similarity. This means that if we change the sizes of the fractal by a several orders of magnitudes comparing with the initial scale or if we take a small part of the fractal it will look exactly the same as the initial object. By saying "look as the initial object" we mean that the new object would have not only a similar geometrical structure but would also have the same statistical properties as the initial fractal. The property of self-similarity could be well demonstrated on the examples of the Cantor Set (fig. 1) and Mandelbrot Set (fig 2). This fractals have been thoroughly studied in mathematics and further details on them could be found in [2] and [3].



Figure 1: The Cantor Set [1].

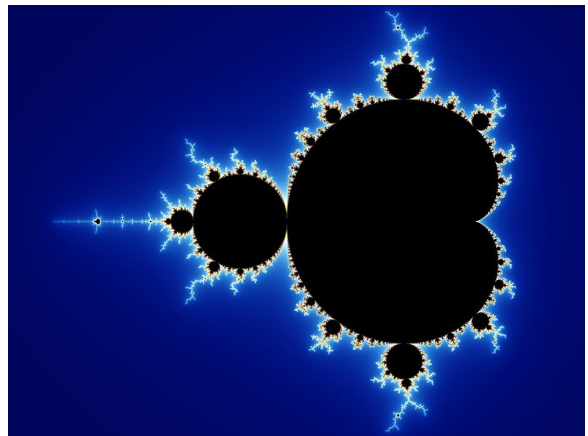


Figure 2: The Mandelbrot Set [1].

The volume of any fractal can be measured by covering it with d dimensional spheres of radius l . We will use notation d for the usual Euclidian dimension. Then we could get the estimate of the fractal volume as:

$$V(l) = N(l)l^d, \quad (1)$$

where $N(l)$ is the smallest number of d dimensional spheres needed to completely cover the fractal object. We assume that l is much smaller than the linear size L of the object. For simple shapes of objects $V(l)$ reaches a constant value independent of l in the limit of infinitely small l . But for the fractals $V(l) \rightarrow 0$ with $l \rightarrow 0$ while the area of a fractal could be infinitely large [4]. Alternatively, to measure the fractal volume we could imagine a d dimensional lattice with lattice spacing l covering the region of a space that contains the fractal. Then $N(l)$ would be a number of all d dimensional boxes of volume l^d that cover the fractal. This method is called box counting.

To demonstrate the two aforementioned features of fractals in a simple way we shall refer to a common example of the shore of England. The curvature of the shore looks approximately the same if being observed from different altitudes. In other words we can see the same structure of the coast if we watch at different scales, which illustrates the self-similarity of the shore. Now if we try to measure the length of the shore we would notice that it increases indefinitely with the decreasing of the magnitudes of the measuring device (fig. 3). But its area tends to decrease and go to zero. Thus, we see that the length of such object is much bigger compared to a line on the same scale and consequently such object is too large to be a one-dimensional line, but, on the other hand, the area of the shore is too small in order it could be a two-dimensional object. Already at this stage we could give a simple definition



Figure 3: Measuring the length of the shore of England. Decrease of the sizes of the measuring devices (spheres) leads to the infinitely large length but infinitely small area [1].

of a fractal. In the most general case any object is a fractal, if it is impossible to get a well converging finite measure for volume, surface or length when changing the linear sizes of the measuring device (d dimensional spheres or boxes) over a several orders of magnitudes [4].

Having an initial object with a given geometrical configuration, basically, there are two possible ways of forming a self-similar fractal either by repeated addition of copies of the initial object (fig. 4 a) or by subsequent division of the initial object (fig. 4 b). In the case of real physical systems there are always restrictions on the maximum and minimum possible scales imposed by the linear sizes of the whole fractal structure and its constituents respectively. Obviously, the most relevant, from a physical point of view, way of self-similar structure formation is the addition of similar objects, since due to this mechanism most of the structures in real physical systems are grown.

As was pointed out above, fractals can not be described by means of usual (integer)

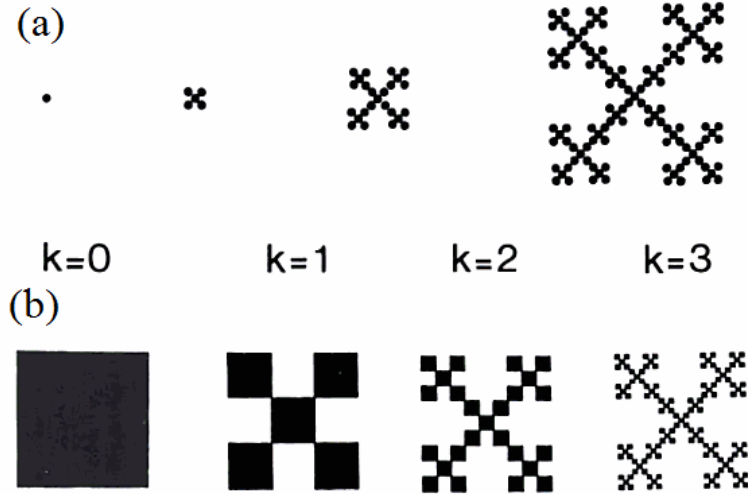


Figure 4: Iterative procedure for generating self similar fractals. (a) Repeated addition and (b) subsequent division of the initial object. k - number of iterations. In the limit $k \rightarrow 0$ we will get mathematical fractal which is infinitely large (a) or infinitely fine (b) [4].

Euclidian dimensions. In general case fractal dimension is noninteger and we shall denote it as D . For the case of growing fractals the volume $V(L)$ is usually considered as function of linear size L of the region of a d dimensional space occupied by a fractal. To compute the volume one usually covers the fractals with d dimensional spheres (of boxes) of a radius l which is set to the smallest typical size of the system (length of the constituent particles). In the units of a such characteristic length the volume will be simply equal to the number of such spheres, $V(L) = N(L)$. Assuming that the object is the mathematical fractal implies that the volume of the object diverges according to a non-integer exponent [4]:

$$N(L) \sim L^D. \quad (2)$$

This relation allows for the defining of the fractal dimension D [4]:

$$D = \lim_{L \rightarrow \infty} \frac{\ln(N(L))}{\ln(L)}. \quad (3)$$

For the fractals generated via subsequent division of the initial object the linear size of the whole structure is fixed but it gets infinitely fine in the limit of infinite number of subdivisions. In such case the number of spheres needed to cover the fractal is considered as a function of the radius of the spheres. Logically, one can write [4]:

$$N(l) \sim l^{-D}, \quad (4)$$

and, consequently, define D as [4]:

$$D = \lim_{l \rightarrow 0} \frac{\ln(N(l))}{\ln(1/l)}. \quad (5)$$

It could be easily shown that both of the aforementioned definitions lead to the integer dimensionality in the case of simple non-fractal objects. Using, for instance, eq. 3 we can also

define the fractal dimension of the fractal depicted at fig. 4 a. In this case we have $N = 5^k$, $L = 3^k$ and $D = 1.465$.

Typically fractals only occupy a negligible fraction of the ambient region in the d dimensional Euclidian space. If characteristic linear size of the ambient volume $V_{ambient}$ is L then its volume could be estimated as L^d . If consider a case of a growing fractal due to the repeated addition of particles of the same characteristic size l , the volume of such fractal $V_{fractal}$ could be estimated using the total number of such particles as $l^d N$ (which is equivalent to the formula 1). Now if to measure L in the units of l we would have:

$$\frac{\ln(V_{fractal})}{\ln(V_{ambient})} \sim \frac{\ln(N)}{d \ln(L)}, \quad (6)$$

and in the limit $L \rightarrow \infty$, this ratio yields:

$$\lim_{L \rightarrow \infty} \frac{\ln(V_{fractal})}{\ln(V_{ambient})} \sim \frac{D}{d}. \quad (7)$$

Giving this relation we could think of the fractal dimension D as of a measure of how efficiently fractal occupies the space.

We will not give here a rigorous definition of the Hausdorff dimension, because it is rather a matter of strict mathematical analysis rather then the current project in computational physics. In fact, for the analysis of real physical systems it is more convenient to use the definition of fractal dimension according to the formula 3. The strict definition of the Hausdorff dimension could be found in many textbooks on the subject (e.g. [3]). We will just outline the main idea behind the Hausdorff approach of treating fractals. As was mentioned above all physical systems have the cutoff of the length due to the finite system size L . This allows for using dimensionless measure of length:

$$\epsilon = \frac{l}{L}, \quad (8)$$

where again l is the radius of the covering spheres. Then in this units formula 2 and formula 4 have the same form:

$$N(\epsilon) \sim \epsilon^{-D}, \quad (9)$$

here $N(\epsilon)$ is the number of d dimension spheres of radius ϵL needed to cover the fractal. Main inconvenience in the dealing with fractals is that fractal volume diverges if measured with spheres with integer dimension. To overcome this obstacle Hausdorff proposed to use the spheres with volume ϵ^D . Another idea of Hausdorff was to find such kind of measure for fractals which would be independent of the resolution of the measurement, ϵ . The Hausdorff measure is given by [4]:

$$F = N(\epsilon)\epsilon^D. \quad (10)$$

F is independent of ϵ only if the dimension of the spheres used for measuring coincides with the fractal dimension D . Ordinary fractals are called those structures which have dimension D defined according to formula 9 smaller than the dimension d of the region of a space containing the fractal. But there are some exceptions, so-called fat fractals that have $D = d$ [4].

One of the possible way of classifying fractals is due to their self-similarity [1]. The strongest type of self-similarity is the exact self-similarity (e.g. Cantor Set depicted at fig. 1).

This type of fractals appears to be completely identical at different scales. This is rather idealistic mathematical fractal model. The second type of fractals are those fractals that demonstrate quasi-self-similarity. This means that at different scales fractal approximately resembles the same geometry and statistical properties (e.g. Mandelbrot Set depicted at fig. 2). And the third type is statistically self-similar fractals. This means that at different scales fractals have only preserved some statistical properties. The statistical self-similarity is the case for the most of the physical systems. One of the ways of forming such clusters is due to the random processes (e.g. Brownian motion and DLA).

2.2 Measuring Fractal Dimension in Computer Simulation

One possible way to calculate the fractal dimension is to make use of a density-density correlation function [4]:

$$C(\mathbf{r}) = \frac{1}{V} \sum_{\mathbf{r}'} \rho(\mathbf{r} + \mathbf{r}') \rho(\mathbf{r}'), \quad (11)$$

where $\rho(\mathbf{r})$ is a local density at the point \mathbf{r} and it is equal to 1 if the point belongs to the fractal object and 0 otherwise. In the case if we have discrete space where the objects can occupy only lattice points $\rho(\mathbf{r})$ is the density at the lattice site with coordinates \mathbf{r} . For the growing fractals, as was mentioned above, the volume V equals to the number of the covering spheres N . According to the definition of the density-density correlation function we can estimate the number of covering spheres (with radius equal to the smallest size of constituent particles) in the d dimensional volume of radius L :

$$N(L) \sim \int_0^L C(\mathbf{r}) d^d r. \quad (12)$$

This expression makes it obvious to think of $C(\mathbf{r})$ as a probability density of finding two points belonging to the fractal at distance \mathbf{r} between each other. Usually the vast majority of ordinary fractals are isotropic, and, consequently the density-density correlation functions depends only on the absolute value of the distance between the particles, $C(\mathbf{r}) = C(r)$. It could be mathematically shown that for the non-trivial self-similar (it better to say self-invariant) objects the density-density correlation function follows the next power law dependency on r [4]:

$$C(r) \sim r^{-\alpha}. \quad (13)$$

Using this power law and formulas 12 and 2 it is straightforward to find the relation between usual Euclidian dimension d , fractal dimension D and the density-density correlation function exponent α :

$$D = d - \alpha. \quad (14)$$

To get α one usually computes the density-density correlation function from the computer simulation data and then defines α via a linear fit of $\ln(C(r))$ as a function of $\ln(r)$.

The alternative way of defining D is to use as the estimate for the measure of the linear size L of the fractal its radius of gyration R_g . Radius of gyration R_g is simply the average distance between points (particles) of the fractal and its center of mass [4]:

$$R_g = \frac{1}{N} \sum_{i=1}^N r_i, \quad (15)$$

where r_i is the distance between the i -th particle of the fractal and its center of mass and N is the total number of particles in the fractal. For the non-trivial self-invariant objects the radius of gyration follows the next power law dependency on N ([4],[7],[9]):

$$R_g \sim N^\beta. \quad (16)$$

Using this power law and the scaling law of the number of particles in the fractal (formula 2) one immediately notices the relation between the fractal dimension and the radius of gyration exponent β :

$$D = \frac{1}{\beta}. \quad (17)$$

And again to get R_g one usually computes the slope from the linear fit of $\ln(R_g)$ as a function of $\ln(N)$. This method is the most frequently used for the diffusion limited aggregation (DLA) clusters, because usually even for comparably small clusters (fractals) there is a sufficient region of values of $\ln(N)$ for which $\ln(R_g)$ resembles very nicely a linear behavior.

In the following in this report we shall denote the fractal dimension computed using the radius of gyration as D_β and the fractal dimension computed using the density-density correlation function as D_α .

2.3 DLA Model

Diffusion limited aggregation (DLA) model was first proposed by Witten and Sander [6] in 1981 and later further developed and implemented by Meakin ([7],[8],[9],[10]) for the computer simulation of fractal formation in systems where mainly diffusion governs the transport of particles. A precondition for such kind of systems is that the concentration of reacting particles has to be low. Diffusion limited aggregation is experimentally observed in a wide range of electrochemical systems (e.g. [13],[14]). Typical DLA fractal clusters are depicted at the figures (5,6,7).

In such systems particle aggregation mainly happens due to the Coulomb and Van der Waals forces. Since the concentration of active particles is low they interact rarely and the cluster growth is mostly due to the adding (via attraction) a single particle to the cluster at a time rather than large agglomerates of particles. As it is seen from figures (5,6,7) the cluster growth preferably happens at the outer regions of the structures. The probability of a particle being stick to a cluster depends on the type of interatomic (or intermolecular) potential. If particle does not stick to the cluster once it has reached it for the first time the particle continues to diffuse in the vicinity of the cluster till it is finally absorbed by the cluster or till it leaves the region of the cluster.

It is possible to describe the DLA growth process analytically. The derivation of differential equation describing DLA could be found in [5], we do not present it in this work, because it is beyond the scope of the current project.

3 Computer Simulation of Fractal Growth

3.1 Irreversible DLA Model of Single Immobile Cluster Formation

3.1.1 Simulation Method

To simulate diffusion limited cluster aggregation process we have followed the model proposed by Witten and Sander[6] and later developed by Meakin ([7],[8],[9]). The model and algorithm

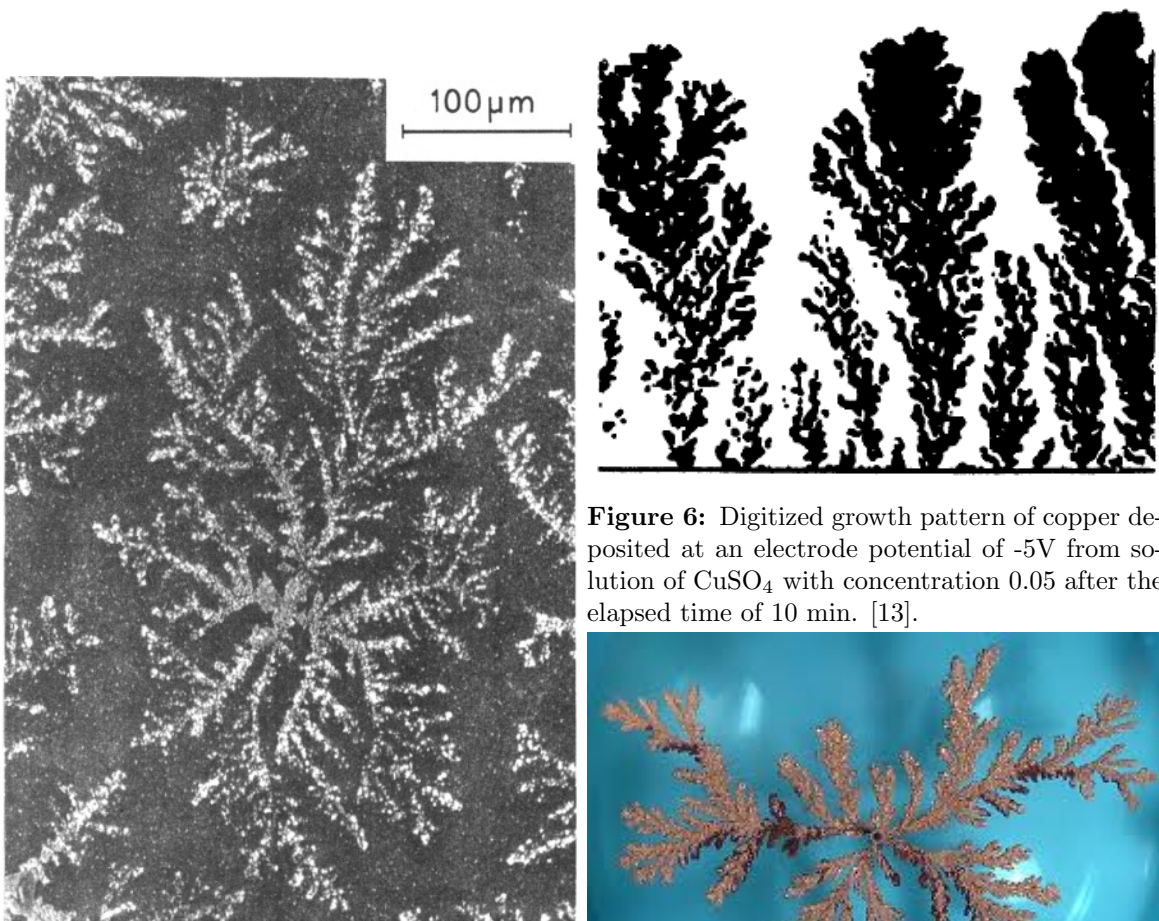


Figure 5: Scanning electron micrograph of a fractal structure formed by evaporating a gold solution on a glass slide. This structure has a fractal dimension of 1.7 [14].

Figure 6: Digitized growth pattern of copper deposited at an electrode potential of -5V from solution of CuSO_4 with concentration 0.05 after the elapsed time of 10 min. [13].



Figure 7: A typical DLA cluster grown from a copper sulfate solution in an electrodeposition cell [1].

are based on the Monte Carlo method. We have used two dimensional simple cubic lattice. Particles are allowed to occupy only the lattice sites. Initially a seed particle is placed in the center of the system. Then the first particle is added to the lattice at sufficiently far distance from the seed and undergoes a random walk over the lattice via successive random jumps to one of the four nearest neighbor sites. Probability of a jump to any of the nearest neighbor sites is the same and normalized in order to have the overall jump probability equal to unity. Once the particle reaches one of the adjacent to the seed sites it could be attached to the seed according to the sticking probability at the first nearest neighbor sites p_{nn} and to the sticking probability at the second nearest neighbor sites p_{snn} . To be more specific, p_{nn} is the probability for moving particle to stick to the cluster if there is one particle that belongs to the cluster at one of the nearest neighbor sites of the moving particle. Consequently, if there are two or more particles belonging to the cluster at the first nearest neighbors of the moving particle then it has higher probability to stick to the cluster. The same explanation is applicable to the p_{snn} with respect to the second nearest neighbor sites. During the simulation

each of the first nearest neighbor sites is checked one after another after each jump. If the moving particle sticks to the cluster at one of the nearest neighbor sites then the checking is stopped. If the particle doesn't stick to any of the nearest neighbor sites, then the second nearest neighbor sites are checked one after another. Such approach is equivalent to the computation of the conditional probabilities for the moving particle to stick at each of the first or second nearest sites, but it rather works faster if implemented in the simulation. So, if the particle sticks to none of the first or second nearest neighbor sites once it hits the cluster for the first time, then it continues the random walk till it will be attached to the cluster or till it moves too far from the cluster. In later case particle is deleted from the lattice ("killed") and starts off again from the closer distance to the cluster. After the first particle is finally attached to the cluster the second particle is introduced to the lattice and undergoes the same procedure. In such way the cluster is formed. We have started off the particles at the

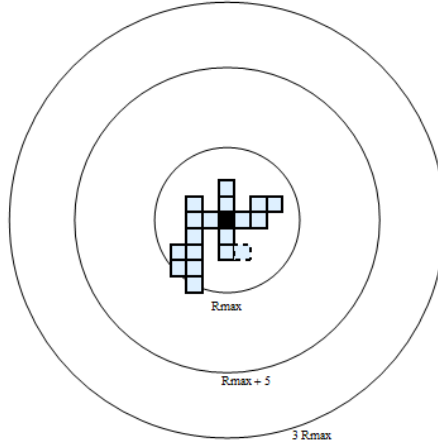


Figure 8: Schematic depiction of the model applied to simulate cluster growth from the initial seed particle.

distance $R_{max} + 5$ from the cluster, where R_{max} is the maximum distance from the seed to the outermost particle in the cluster and all the distances are measured in the units of the lattice spacing. If the particle moves further than $3R_{max}$ from the cluster, it is killed and started off again at random position on the circle of radius $R_{max} + 5$ centered at the same point with the seed particle. Schematic depiction of this system can be found at the figure (8). We have used different values for the radius of the start off circle and for the distance at which particle is killed. And the corresponding results were the same within a statistical error. To decrease the computational time the checking of the first and second nearest neighbor sites is started if the particle reaches the distance $R_{max} + 2$ from the cluster.

3.1.2 Results for Two-Dimensional Clusters

We shall start with a discussion of the simplest for the implementation case of $p_{nn} = 1$. Typical fractal clusters formed under such condition are demonstrated at the figure (9) and at the figure (44) from appendix A. One can notice from these figures that such type of clusters posses quite a loose structure, because the cluster growth happens mostly at the outer regions of the structure, since a wandering particle has a higher probability of crossing large branches of the cluster rather than penetrating into the inner region. Figures (13,14) demonstrate that

the cluster density decreases from the center of the cluster towards its outer regions. Despite of the substantial random fluctuations one could notice that the density as the function of a distance from the center of the cluster continuously falls without regions of constant density. Figure (14) demonstrates how random fluctuations could be reduced via averaging over several clusters. One could expect that the density drops according to the same power law as the density-density correlation function which reveals the essential fractal nature of the DLA clusters. We have computed the density-density correlation function which is shown at the figure (11). $\ln(C(r))$ shows approximately linear dependency on $\ln(r)$ and constant slope over the region of $0 < \ln(r) < 4.5$. This indicates that our results are consistent with formula (13) and we have $C(r) \sim r^{-\alpha}$. In order to compute $C(r)$ one normally calculates the number of particles at distance r from the reference particle for the all particles in the cluster and then normalizes it using the total number of particles and the corresponding volume between two spheres of radius $(r - \delta r)$ and $(r + \delta r)$ respectively. We have used the value 0.5 for the δr .

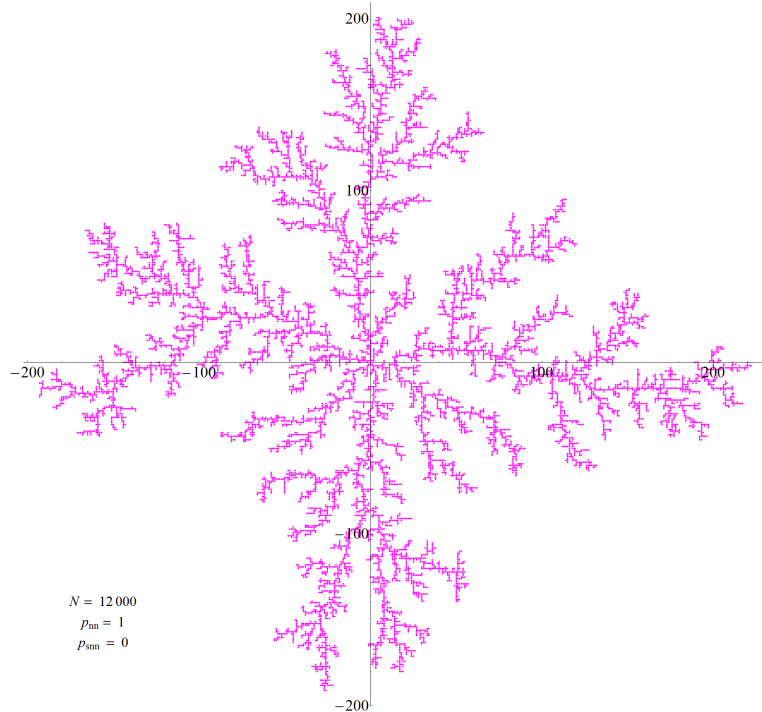


Figure 9: Typical two dimensional cluster of $N = 12000$ particles obtained from the Monte Carlo simulation of DLA growth from the seed particle fixed in the center of the system. Sticking probability at the nearest neighbor sites p_{nn} is 1.

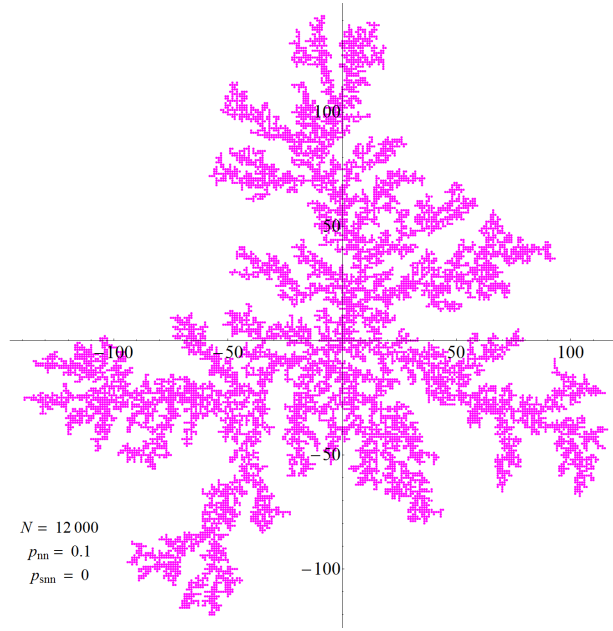


Figure 10: Typical two dimensional cluster of $N = 12000$ particles obtained from the Monte Carlo simulation of DLA growth from the seed particle fixed in the center of the system. Sticking probability at the nearest neighbor sites p_{nn} is 0.1.

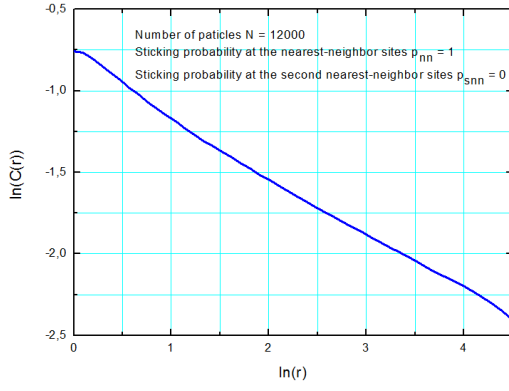


Figure 11: Double logarithmic plot of the density-density correlation function for the DLA cluster of $N = 12000$ particles and sticking probability at the nearest neighbor positions p_{nn} equal to 1. The plot is received via averaging over 15 clusters.

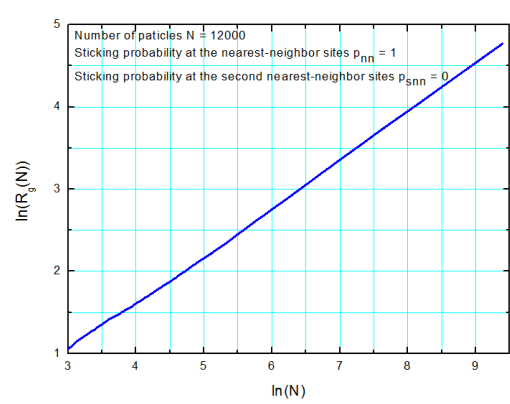


Figure 12: Double logarithmic plot of the radius of gyration for the DLA cluster of $N = 12000$ particles and sticking probability at the nearest neighbor positions p_{nn} equal to 1. The plot is received via averaging over 15 clusters.

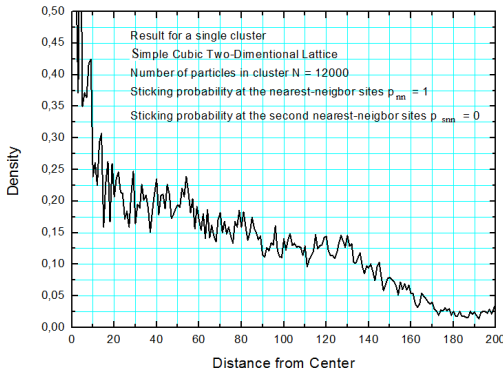


Figure 13: Density distribution from the center of the DLA cluster of $N = 12000$ particles and sticking probability at the nearest neighbor positions p_{nn} equal to 1. The plot for a single cluster.

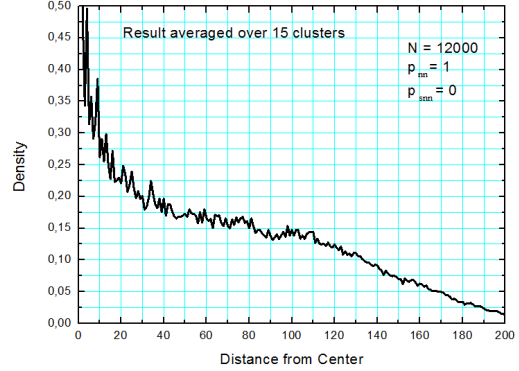


Figure 14: Density distribution from the center of the DLA cluster of $N = 12000$ particles and sticking probability at the nearest neighbor positions p_{nn} equal to 1. The plot is received via averaging over 15 clusters.

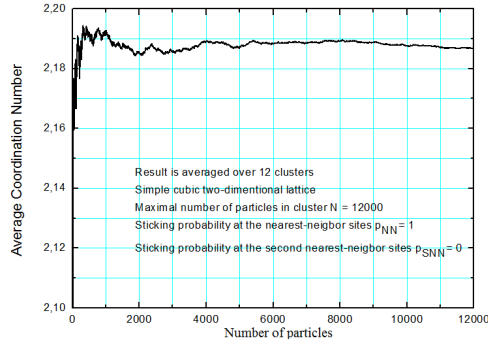


Figure 15: Coordination number for the DLA cluster of 12000 particles and $p_{nn} = 1$.

The radius of gyration R_g computed in our simulations for the case of $p_{nn} = 1$ also demonstrates expected power law dependency $R_g \sim N^\beta$ (fig. 12).

The density-density correlation exponent α and the radius of gyration exponent β were calculated as was discussed in section 2.2. We also want to draw your attention that for the fitting procedure we have created or own fitting C++ program, which is based on the least square method and is able to perform a fit with a polynomial of any desired power. The results for the case of $p_{nn} = 1$ for the α , β and the average coordination number (the average number of the nearest neighbor sites) are given in the table (1) and for the corresponding fractal dimensions D_α and D_β in the table (2).

The results from the tables (1,2) are the same (within statistical error) for the clusters of different numbers of particles N . Which points out that for the cluster sizes used in the simulations scaling effects are negligible. Both fractal dimensions D_α and D_β seem to oscillate around the same value of ≈ 1.7 , which is smaller than the ambient Euclidian dimension $d = 2$. One remark could be made concerning D_α in the cases of $N = 50000$ and $N = 100000$, in this cases $D_\alpha \approx 1.67$ which (even within its error) is smaller than 1.7. But to make any conclusions regarding the overall behavior of D_α for large clusters (if it tends to decrease) one needs bigger statistics.

N	Radius of gyration exponent, β				Density-density correlation function exponent, α	Coordination number
	50% ^a	75% ^b	90% ^c	95% ^d		
12000	0.59448±0.04386	0.58972±0.03431	0.5845±0.0281	0.5844±0.0305	0.3088±0.063	2.1855±0.0049
15000	0.5935±0.0243	0.598±0.0232	0.5971±0.0192	0.5959±0.019	0.313±0.048	2.1846±0.0096
17000	0.5881±0.0389	0.584±0.038	0.5822±0.0322	0.5833±0.0299	0.309±0.035	2.1845±0.0064
20000	0.5889±0.0386	0.5882±0.0383	0.5836±0.0306	0.5822±0.0249	0.3176±0.0322	2.186±0.007
50000	0.5897±0.0254	0.5908±0.0159	0.5917±0.0143	0.59±0.015	0.3259±0.0252	2.1837±0.0055
100000	0.587 ±0.029	0.5866 ±0.0299	0.587 ±0.021	0.5873 ±0.0177	0.326 ±0.017	2.1857 ±0.0024

Table 1: Results obtained from the simulation of DLA cluster formation on two dimensional simple cubic lattice with a sticking probability at the nearest neighbor sites $p_{nn} = 1$ and at the second nearest neighbor sites $p_{snn} = 0$. N is the total number of particles in the final cluster. ^a - Radius of gyration exponent computed using last 50% of particles added to cluster, ^b, ^c and ^d - correspond to the radius of gyration exponent computed using last 75%, 90% and 95% of particles added to cluster respectively. All values of α , β and coordination number are averaged over 10 clusters.

N	D_β				D_α
	50%	75%	90%	95%	
12000	1.6822±0.1241	1.6957±0.0987	1.711±0.0824	1.7112±0.0894	1.6912±0.063
15000	1.685±0.069	1.6722±0.0648	1.6749±0.0539	1.6783±0.0535	1.687±0.048
17000	1.7005±0.1126	1.7126±0.1114	1.7178±0.0949	1.7144±0.0878	1.691±0.035
20000	1.698±0.111	1.7003±0.1108	1.7135±0.0897	1.7176±0.0734	1.6826±0.0322
50000	1.696±0.073	1.693±0.046	1.69±0.041	1.6948±0.0422	1.6741±0.0252
100000	1.7038 ±0.0841	1.7047 ±0.0868	1.703 ±0.061	1.7027 ±0.0512	1.674 ±0.017

Table 2: Fractal dimension computed from the radius of gyration and density-density correlation function given in table (1).

One could also notice from the tables (1,2) that for the large clusters ($N = 50000$) we have smaller errors.

From the figure (15) one could notice that the average coordination number tends to the constant value in the limit of large N .

In the case of the small sticking probability at the nearest neighbor sites clusters get more dense. For instance, it could be seen from the figure (10) for the case of $p_{nn} = 0.1$. The results for the α , β , average coordination number, D_α and D_β in the case of $p_{nn} < 1$ could be found in appendix B (tabs. 5,6). Surprisingly, but it appears to be that density-density correlation function exponent and radius of gyration exponent along with corresponding fractal dimensions remain essentially the same within statistical error for the range [0.1 – 1.0] of the sticking probability at the nearest neighbors, whereas, as expected, the average coordination numbers increases with the decrease of the p_{nn} .

In the case of zero sticking probability at the nearest neighbor sites but nonzero sticking probability at the second nearest neighbor sites the clusters become much more looser and have more transparent structure, which occupies the larger region of space compared to the corresponding clusters with $p_{nn} \neq 0$ and the same number of particles (fig. 16,17). The results for the α , β , average coordination number, D_α and D_β in the case of $p_{snn} \neq 0$ and $p_{nn} = 0$ could be found in the appendix C (tabs. 7,8). In these results we have again approximately the same values for the exponents and fractal dimensions for different values of p_{snn} , and, in addition, their values (within statistical error) are same as for the case of nonzero p_{nn} . These results confirm Meakin's outcome [7], which was received with a very poor statistics for averaging.

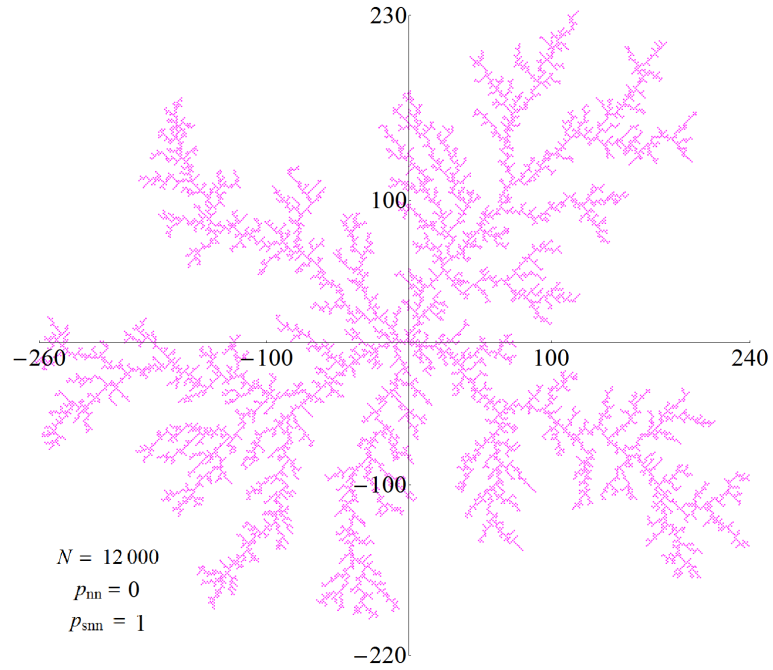


Figure 16: Typical two dimensional cluster of $N = 12000$ particles obtained from the Monte Carlo simulation of DLA growth from the seed particle fixed in the center of the system. Sticking probability at the second nearest neighbor sites p_{snn} is 1.

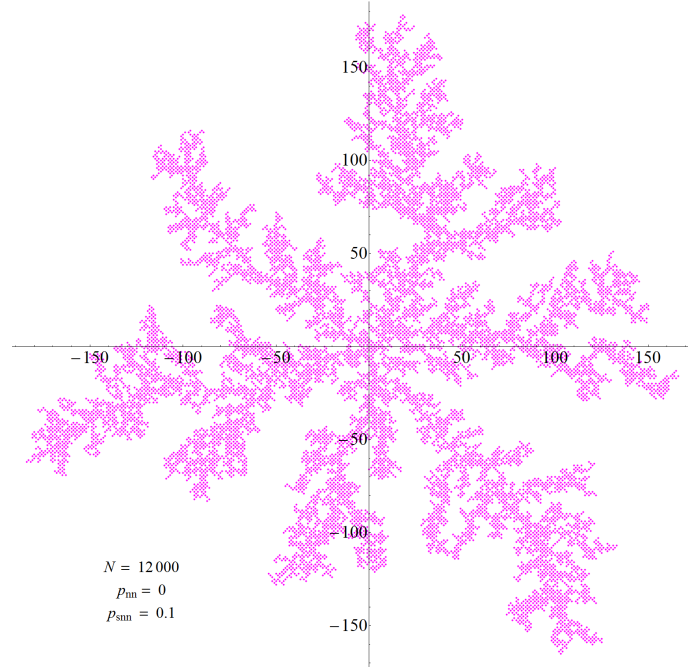


Figure 17: Typical two dimensional cluster of $N = 12000$ particles obtained from the Monte Carlo simulation of DLA growth from the seed particle fixed in the center of the system. Sticking probability at the second nearest neighbor sites p_{snn} is 0.1.

We have also computed α , β , average coordination number, D_α and D_β for the case when p_{nn} and p_{snn} are simultaneously nonzero. The results are given in the appendix D (tab. 9,10 and fig. 49,50).

3.1.3 Results for Three-Dimensional Clusters

To simulate DLA cluster formation in 3D space we have followed exactly the same simulation method as for the 2D case. The density-density correlation function for the case $p_{nn} = 1$ is shown at the figure (18). $\ln(C(r))$ resembles approximately linear behavior over the range (0 – 3) for the values of $\ln(r)$ which makes possible the determination of the density-density correlation function exponent α . Meakin [7] has received far from linear behavior for $\ln(C(r))$ and claimed that α and respectively D_α are strongly dependent on the size of clusters used in his work without giving any qualitative and numerical evidences. In Meakin's work the size of the 3D clusters ranges from 6608 to 15000 particles. We shall examine this statement in this section of our report.

The radius of gyration R_g (fig. 19) demonstrates essentially the same power law dependency as for the 2D case.

Typical 3D DLA clusters grown from a seed particle fixed in the center of the system for the case $p_{nn} = 1$ are shown at the figures (20,21). The figure (21) has a very nice perspective which shows that the 3D DLA cluster growth preferably happens at the outer parts of the cluster branches, which leads again to the spacious branch structure, which results in the small volume occupied by the cluster compared to the volume of the ambient space in which the cluster resides. To confirm this observation we have computed the cluster density (fig. 22) and the number of particles (fig. 23) as the functions of the distance from the center of the cluster for different stages of the cluster growth.

From figure (25) shows that the average coordination number attains constant value in the limit of large number of particles, just like in the 2D case, though this value is bigger than the corresponding 2D value. This is explained by the fact that in the three dimensional lattice each site has bigger number of the nearest neighbor sites.

One useful quantity which could be computed from the simulation data and give important information on the fractal properties of the object [2] is the projected area $P(N)$ of the object onto 2D planes. Figure (24) demonstrates that $P(N)$ follows the next power law $P(N) \sim N^\gamma$. Projected area exponent γ could be calculated via linear fit of the $\ln(P(N))$ versus $\ln(N)$.

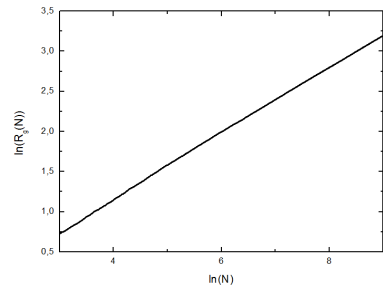
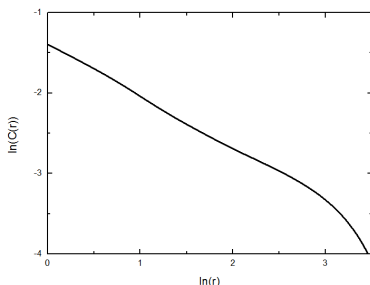


Figure 18: Double logarithmic plot of the density-density correlation function $C(r)$ for the dius of gyration R_g for the DLA 3D cluster of $N = 8000$ particles. $p_{nn} = 1$. $N = 8000$ particles. $p_{nn} = 1$. The plot is received via averaging over 10 clusters. received via averaging over 10 clusters.

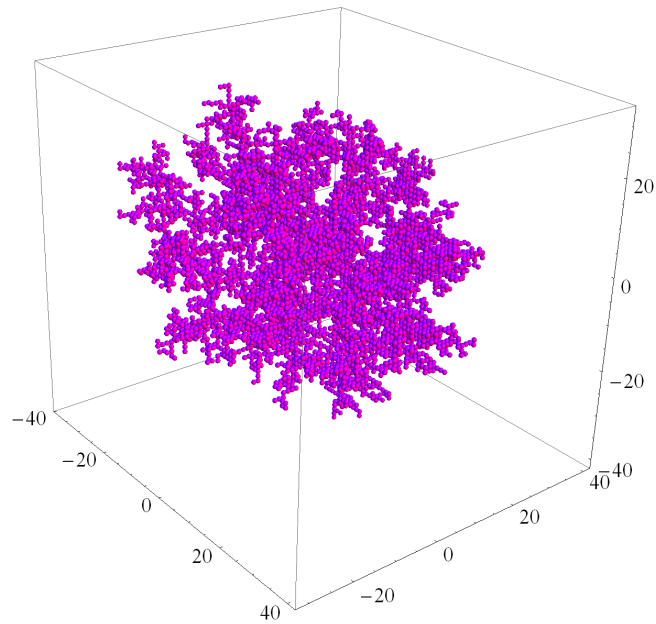


Figure 20: Typical three dimensional cluster of $N = 8257$ particles obtained from the Monte Carlo simulation of DLA growth from the seed particle fixed in the center of the system. $p_{nn} = 1$.

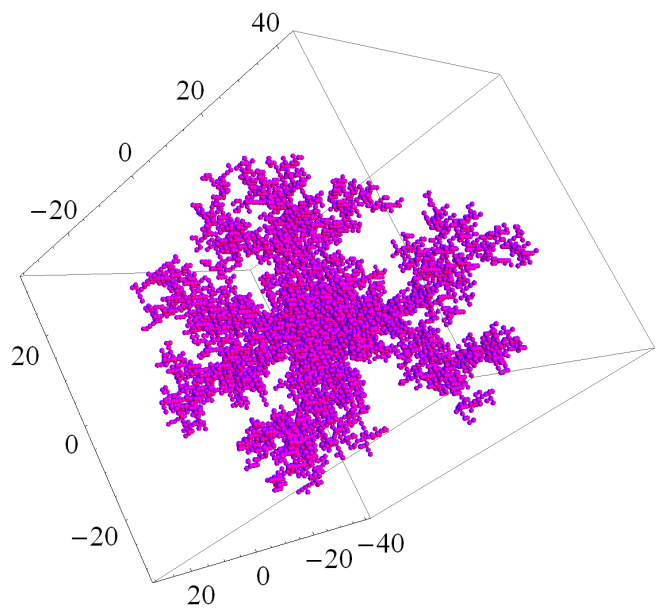


Figure 21: Typical two dimensional cluster of $N = 7762$ particles obtained from the Monte Carlo simulation of DLA growth from the seed particle fixed in the center of the system. $p_{nn} = 1$.

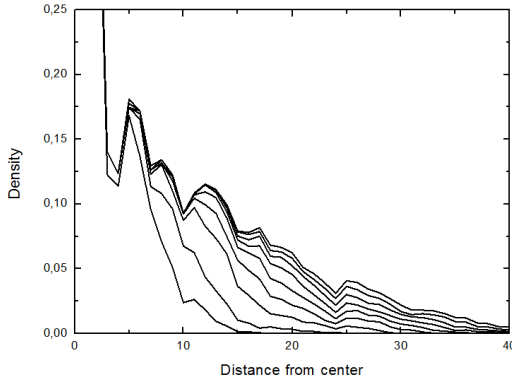


Figure 22: The density distribution as the function of a distance from the center of the 3D DLA cluster at stages where the cluster has grown to a size of 500,1000,...,8000 particles. $p_{nn} = 1$.

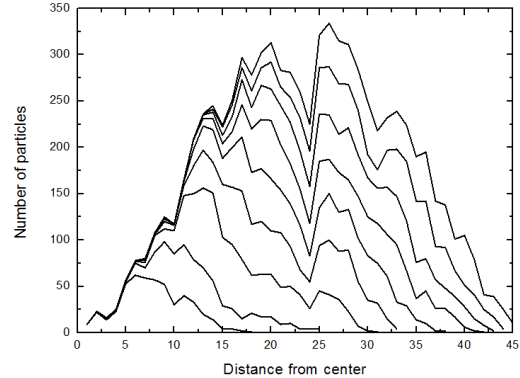


Figure 23: The number of particles as the function of a distance from the center of the 3D DLA cluster at stages where the cluster has grown to a size of 500,1000,...,8000 particles. $p_{nn} = 1$.

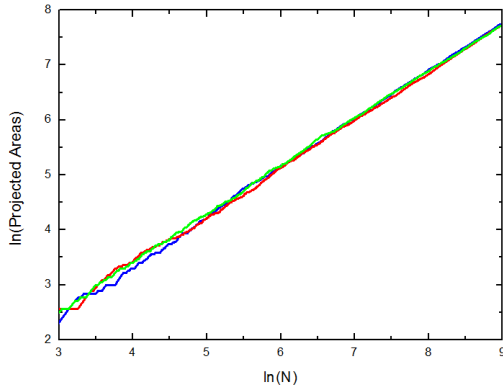


Figure 24: The double logarithmic plot of the projected areas on three mutually perpendicular planes, calculated during the growth of the 3D DLA cluster of the total final size $N = 7870$ particles. $p_{nn} = 1$.

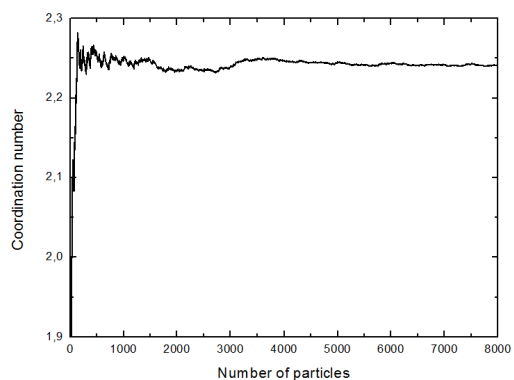


Figure 25: The average coordination number calculated during the growth of the 3D DLA cluster of the total final size $N = 8000$ particles.

The results for the β , α , D_β and D_α and values of the projected area exponent are given in the table (3) for the case $p_{nn} = 1$. From this data one notices that values of D_β for different sizes of the clusters are essentially the same (of course within the statistical error) and oscillate around 2.5. The values of D_α for different sizes of the clusters are also essentially the same (within the statistical error) and oscillate around 2.4. And the values of γ are the same for different sizes of the clusters as well. Our results show that α and, respectively, D_α do not depend drastically on the size of the clusters used in the current project (in the contrast to the Meakin's statement [7]). These results might be due to the larger (better) statistics used in the present study compared to the one used by Meakin. Based on the aforementioned results, we come to a conclusion that the density-density correlation function could be also used (along with R_g) for the calculation of the fractal dimension in the 3D case for clusters of similar or larger sizes compared to those used in our simulations, of course reasonable statistics for the averaging is required.

N	Radius of gyration exponent, β				α
	50%	75%	90%	95%	
8000	0.40056±0.01594	0.39860±0.01833	0.39907± 0.01679	0.39983±0.01680	0.61201±0.06811
9000	0.40458±0.02494	0.40475±0.02526	0.40570± 0.02829	0.40636±0.02894	0.61600±0.03668
10000	0.40563±0.02076	0.40016±0.01736	0.39857± 0.01974	0.39931±0.02258	0.58425±0.08868
11000	0.40124±0.03336	0.39762±0.02085	0.39757± 0.01785	0.39722±0.02002	0.56287±0.04236
12000	0.39605±0.01808	0.39444±0.02144	0.39788± 0.02113	0.39904±0.02017	0.55378±0.07145
13000	0.40480±0.01951	0.39838±0.01771	0.39840± 0.01898	0.40049±0.02044	0.56125±0.06310
14000	0.40435±0.02046	0.40398±0.01694	0.40363± 0.01620	0.40310±0.01563	0.55598±0.06643
15000	0.40051±0.01778	0.40048±0.02798	0.39840± 0.02741	0.39757±0.02221	0.54841±0.07530
N	D_β				D_α
8000	2.49652±0.09935	2.50879±0.11540	2.50585± 0.10543	2.50104±0.10509	2.38800±0.06811
9000	2.47169±0.15239	2.47067±0.15416	2.46489± 0.17188	2.46090±0.17526	2.38400±0.03668
10000	2.46529±0.12617	2.49901±0.10845	2.50899± 0.12423	2.50429±0.14161	2.41575±0.08868
11000	2.49227±0.20721	2.51493±0.13187	2.51529± 0.11290	2.51749±0.12685	2.43713±0.04236
12000	2.52494±0.11527	2.53523±0.13784	2.51334± 0.13344	2.50603±0.12670	2.44622±0.07145
13000	2.47038±0.11910	2.51013±0.11159	2.51007± 0.11955	2.49697±0.12741	2.43875±0.06310
14000	2.47310±0.12511	2.47537±0.10380	2.47750± 0.09940	2.48077±0.09616	2.44402±0.06643
15000	2.49683±0.11087	2.49699±0.17449	2.51007± 0.17273	2.51526±0.14048	2.45159±0.07530
N	Projected area exponent, γ				
8000	0.85676±0.05622	0.85518±0.05796	0.85829± 0.04623	0.86039±0.04550	
9000	0.87372±0.04572	0.86251±0.02926	0.86622± 0.02553	0.86956±0.03268	
10000	0.86066±0.05705	0.86370±0.02762	0.86015± 0.02105	0.85919±0.02266	
11000	0.86287±0.07245	0.86138±0.04181	0.86320± 0.04360	0.86445±0.03482	
12000	0.87847±0.04246	0.86522±0.03623	0.86390± 0.02893	0.86393±0.02989	
13000	0.86198±0.05392	0.86317±0.03646	0.86629± 0.02850	0.86815±0.02438	
14000	0.84946±0.03711	0.85261±0.03292	0.85813± 0.02162	0.86226±0.02274	
15000	0.84835±0.03063	0.84973±0.02588	0.85554± 0.02107	0.85917±0.01821	

Table 3: Results obtained from the simulation of DLA cluster formation on the three dimensional simple cubic lattice. $p_{nn} = 1$. All values of α , β , D_α , D_β and γ are averaged over 10 clusters.

We also want to notice that in the Meakin's work [7] the errors for the values of α , β , D_α , D_β and γ look suspiciously small which might be due to the possible low quality of the random number generator (which might gave all the time very close correlated values) used by Meakin.

In the case of small sticking probabilities the clusters become more dense. For instance, it could be seen from the figure (55) from the appendix E, which shows the typical 3D DLA cluster grown from a seed particle fixed in the center of the system in the case of $p_{nn} = 0.25$. The results for the computed values of the radius of gyration exponent β , the density-density correlation function exponent α , the corresponding values of the fractal dimensions D_β and D_α and values of the projected area exponent are given in the table (11) from the appendix E for the case $p_{nn} = 0.25$. Again in average the values of D_β oscillate around 2.5 and do not depend on the cluster size. The values of D_α show the tendency to the negligible increase with the increase of the cluster size, but giving the magnitudes of the statistical error this is rather a blurred speculation than a solid fact. The values of γ demonstrate slight dependency on the value of the sticking probability. For the case of $p_{nn} = 0.25$ γ oscillates in average around the value of 0.82, whereas, in the case of $p_{nn} = 1$ γ oscillates in average around the value of 0.86.

3.2 Irreversible DLA Model of Multiple Mobile Clusters Formation

With our first programm we could simulate the growth of a cluster by adding particles to a lattice site, then performing random walk and finally getting stuck to a fixed particle in the center of our lattice. This programm was based on the article of Paul Meakin [10]. Now we want to simulate the motion of many particles on a lattice building clusters as they hit each other. This model is as one can imagine already close to the physical reality of real particles performing brownian motion. The algorithm and the measurement of fractal dimension is inspired by the article [10] also by Paul Meakin.

3.2.1 Simulation Method

In the beginning many particles are distributed randomly to different sites on a twodimensional lattice. The periodic boundary conditions are used. When two particles have a distance of one lattice unit (nearest neighbors) they stick to each other forming a cluster. (In the following we will not differentiate between single particels and clusters anymore but call them both clusters. A single particle in our programm means a cluster containing only particle.) Now the following steps are performed:

1. One of the clusters is picked at random. For the chosen cluster one step in a random direction is performed.
2. For the new position of the cluster a check for nearest neighbours is performed i.e. for every particle in the cluster the nearest neighbor sites are checked.
3. If there is a particle of a different cluster at a nearest neighbor position of the first cluster, both clusters are merged and move as one cluster from now on.

These steps are permanently repeated until there is only one big cluster left in the end and the programm stops.

The probabiltiy of clusters getting stuck to each other is highest at the outer region of each cluster. So for a high number of particles and small enough densities the cluster that is formed in the end of the programm should show a fractal structure.

3.2.2 Results

Like in the article of Meakin, we tried to calculate the movement of particles on a twodimensional cluster for four different densities.

$$\rho = \frac{\text{number of particles}}{\text{number of lattice sites}}$$

$$\begin{aligned}\rho_1 &= 0.0625 \\ \rho_2 &= 0.09375 \\ \rho_3 &= 0.125 \\ \rho_4 &= 0.15625\end{aligned}$$

Our programm needed very much RAM to simulate many particles. Thats why we couldn't simulate more then 15000 particles. So to reach higher densities instead of increasing the

particle number we reduced the lattice size. We also made a programm that needed less RAM and could simulate much more particles but until the moment of completion of this report it was still very slow. Our results are depicted in Fig.(26,27,28 and 29)

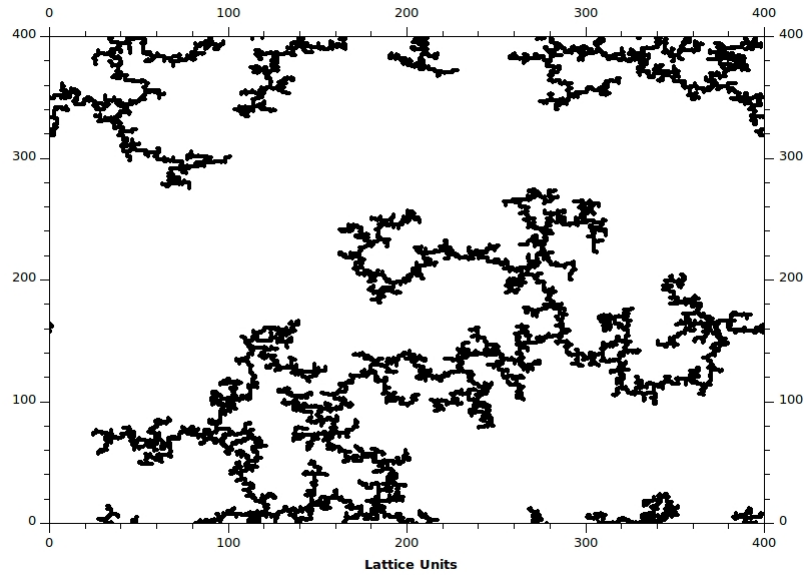


Figure 26: 10 000 particles on a 400×400 lattice corresponding to ρ_1

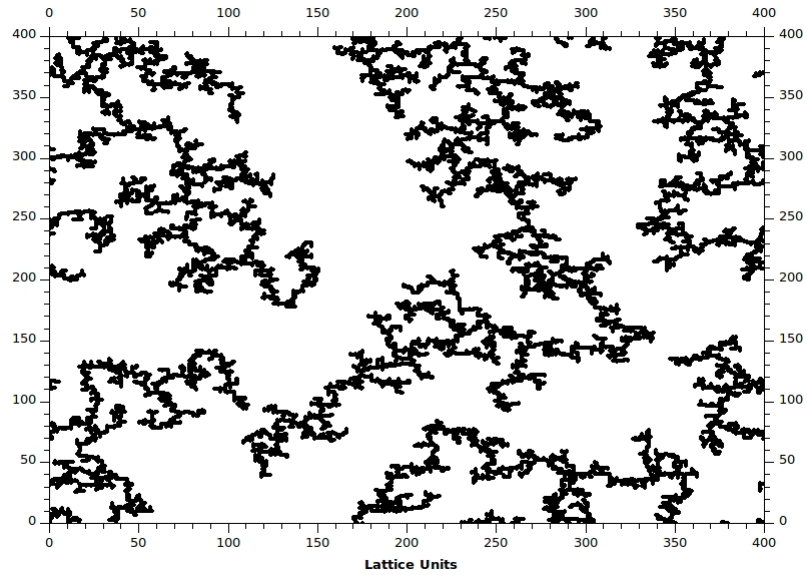


Figure 27: 15 000 particles on a 400×400 lattice corresponding to ρ_2

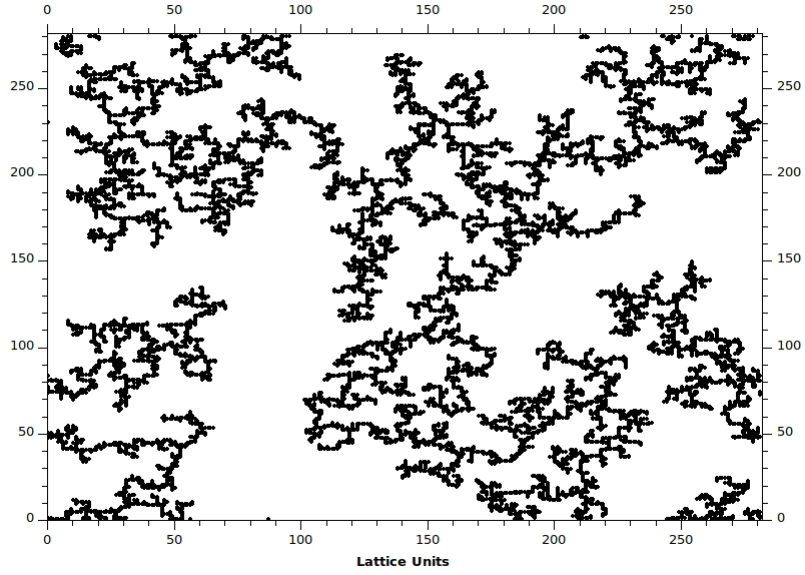


Figure 28: 10 000 particles on a 282×282 lattice corresponding to ρ_3

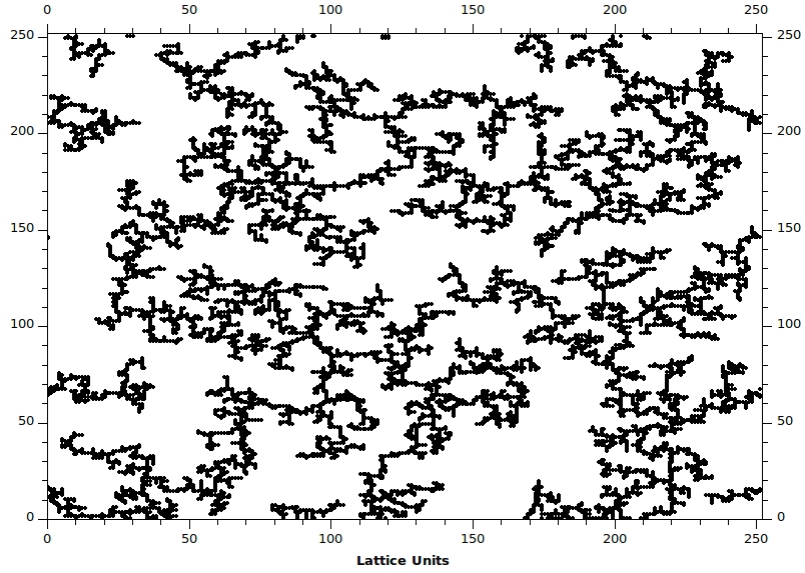


Figure 29: 10 000 particles on a 252×252 lattice corresponding to ρ_4

As one can see the particles indeed form clusters with fractal structure. Fig.(30) shows the self-similarity property of the fractals by showing different zoomed cutouts of Fig.(26).

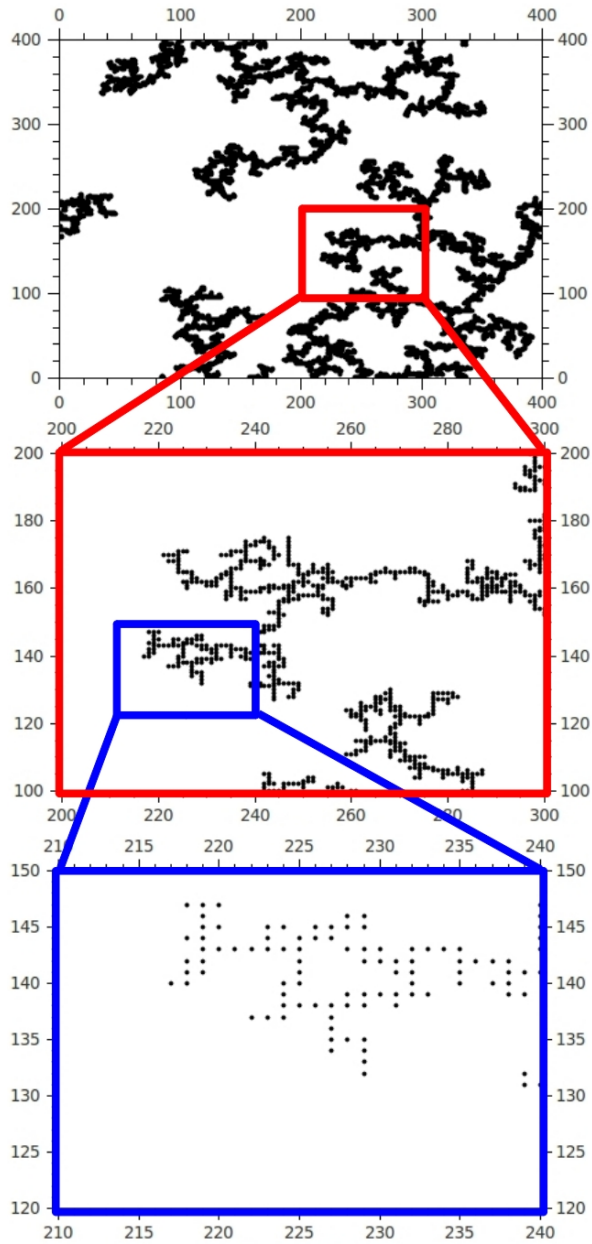


Figure 30

Next we want to calculate the fractal dimension from the density-density correlation functions corresponding to Fig.(26,27,28 and 29). The results are depicted in Fig.(31)

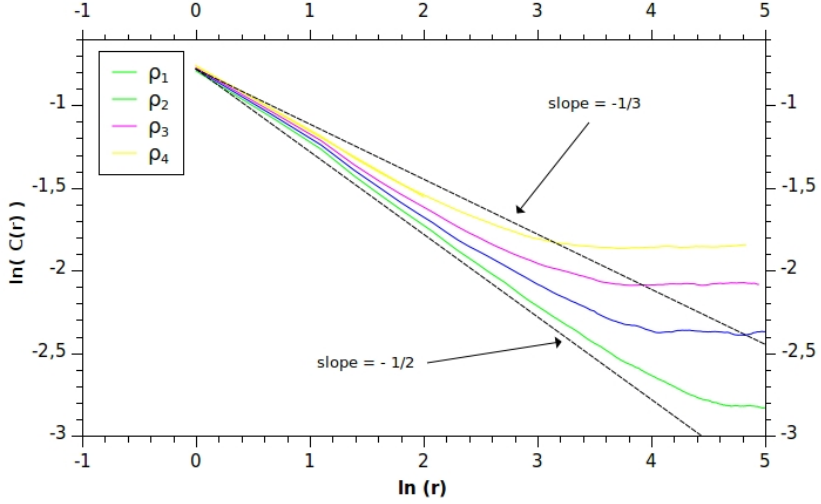


Figure 31: density-density correlation functions obtained for different particle concentrations

These results are an average over 10 simulations. The straight line is a fit of the linear part of the density-density correlation function. The slope of the fitted line yields us the fractal dimension D_α of the fractals, hence:

$$C(r) \approx r^{-\alpha} \quad (18)$$

$$\Leftrightarrow \ln(C(r)) = -\alpha \cdot \ln(r) \quad (19)$$

$$\Rightarrow D_\alpha = d - \alpha \quad (20)$$

Our results for D_α can be seen in table 4. They are consistent with the results obtained by Meakin in [10].

Density	Slope of $C(r)$	Fractal dimension
ρ	α	D_α
$\rho_1 = 0.0625$	0,48	1,52
$\rho_2 = 0.09375$	0,43	1,57
$\rho_3 = 0.125$	0,42	1,58
$\rho_4 = 0.15625$	0,40	1,60

Table 4

3.3 Adaptive Growth Model

3.3.1 Simulation Method

In this section we are going to investigate an adaptive network growth. Adaptive network growth usually takes place in systems which do not grow indefinitely but evolves towards a steady state regime by means of addition and deletion of particles in the cluster. This ability to remove or add particles governs the adaptive nature of the cluster.

We will follow the simulation method of the adaptive network growth based on the Eden model [11] and implemented in one of the Meakin's work [12]. The original Eden model was initially developed to study the growth of biological cell colonies. In this original model particles are not allowed to be removed from the cluster, consequently the cluster could only grow till there are left available particles in the system. The growth process is simulated via adding new particles at randomly selected unoccupied sites on the perimeter of a growing cluster with probabilities that are proportional to the number of occupied nearest neighbors. Such an approach for the growth process leads to the formation of dense structures (appendix F fig. 56) with rough (self-affine) surfaces.

In order to allow for the steady state to be possible an additional variable σ_i (counter) is associated to each particle in the cluster. We will call this variable a "score". After an unoccupied site on the perimeter of the cluster is chosen and a new particle is introduced at this site, the path between newly added particle and the seed particle in the center of the cluster is computed. Then the score σ_i of each particle in this path is increased by an amount δ_1 :

$$\delta_1 = \frac{1}{(1+l)^\eta}, \quad (21)$$

where l is the length of the path and η is a parameter of the model. Once the score for the particles in the path was increased the score associated with all particles is decreased by an amount δ_2 :

$$\delta_2 = \frac{1}{N_m}, \quad (22)$$

where N_m is a parameter of the model. If the score σ_i associated with the i -th particle becomes less than zero, then this particle is removed from the cluster.

In such way the score provides a measure of the degree of participation of the site (occupied by a particle from the cluster) in the growth process and also a measure of "how old is the particle".

There are basically two options to calculate the path between the newly added particle and the seed particle. The first way is to compute the shortest path. For the computation of the shortest path between two points of the lattice one could use, for example, the Lee algorithm. According to the Lee algorithm one starts with the initial site and labels all its nearest neighbors with the number (which is distance between them and initial site), after that one proceeds with the nearest neighbors of already labeled sites and label them again with the number which is distance from this newly labeled sites to the initial one. And one proceeds in such manner till the final destination site will be reached. The second way is what follows. After a new particle is added one could randomly select one of the occupied nearest neighbor sites and assign it as a "parent" site for the newly added particle. In such way a random path between the newly added particle and the seed particle is built up. We have examined both options. In the case of determining the path between the newly added particle and the seed particle as the the shortest path between them on the lattice, one

gets strongly correlated structure of the clusters (appendix F fig. 57). This is why we have used the second way of determining a random path in the further simulations. Interestingly, Meaking has mentioned in his paper [12] that he has used the shortest path between newly added particles and a seed particle in his simulations of the adaptive growth model based on the DLA model.

3.3.2 Results

The typical cluster generated using the aforementioned method using $\eta = 1$ and $N_m = 102400$ is shown at the figure (32). We denote the number of particles added to the cluster as t . The total number of particles added to the cluster depicted at the figure (32) is $t = 2.5 \times 10^5$. The number t of added particles could be used as the measure of the elapsed time. Most of the added particles were subsequently removed and the cluster reaches a steady state regime at which the number of particles in the cluster oscillates around the value of ≈ 7400 particles. The cluster has looser structure towards the outer regions and denser structure towards its center. This is due to that particles which have higher score are located in the inner part of the cluster. To demonstrate this we have depicted particles with different values of the score with different colors (fig. 33). Particles which have the highest score (≥ 250) have magenta color, particles which have the score in the range of values between 70 and 250 are red and so on. The particles with the smaller score are situated on the branches comprised of the particles with the large score. In order to illustrate the cluster structure more clearly we have plotted only those particles which have the score ≥ 100 (fig. 34), and only those particles which have the score ≥ 10 (fig. 35), and only those ones with the score ≥ 1 and score ≥ 0.1 (figures 36 and 37 respectively).

Figure (38) shows the evolution for the two clusters at $\eta = 1$. In the beginning the value of N_m is fixed at the value of 102400 for the first cluster (curve A), and at value of 1600 for the second cluster (curve B). At the early stages of growth the logarithm of the cluster size $S(t)$ increases linearly as a function of $\ln(t)$. Later the steady state is reached at which the cluster size $S(t)$ oscillates around a constant value. After 2.5×10^5 particles were added the value of N_m for the first cluster is switched to 1600 and for the second cluster to 102400 and the clusters are let to evaluate for another 7.5×10^5 steps. Figure (38) illustrates the adaptive nature of the current model. After the value of N_m was changed for the second cluster it quite rapidly reaches a new steady state, which is the same as for the first cluster for $t \leq 2.5 \times 10^5$. And the first cluster after the change of the N_m also tends to attain a new steady state which resembles the steady state of the second cluster before the change of N_m .

Figures (39) and (40) illustrate how different values of the N_m influence on the steady state value of the cluster size $S(\infty)$ for the cases of $\eta = 0$ and $\eta = 2$, respectively. We have also plotted $\ln(S(\infty))$ versus $\ln(N_m)$ for the case $\eta = 2$ (fig. 41). This figure shows that in the steady state the cluster size follows the next power law:

$$S(\infty) \sim N_m^\nu. \quad (23)$$

We have estimated the value of ν for the case $\eta = 2$ which yields the value of 0.55361 ± 0.0132 which is quite close to the one received by Meakin [12].

Comparing figures (42) and (43) one could notice that the model parameters η and N_m strongly influence not only the steady state size of the cluster, but also its structure and density.

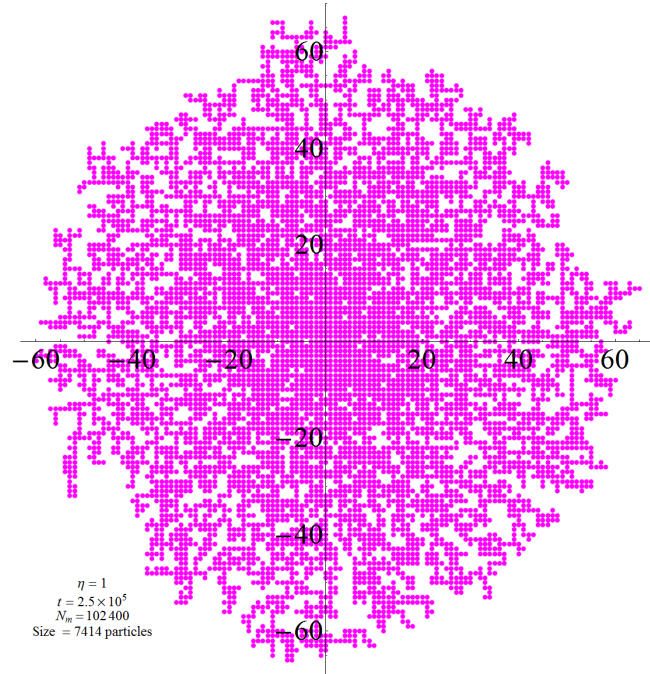


Figure 32: Typical cluster of the adaptive growth model generated with $\eta = 1$ and $N_m = 102400$ after the addition of $t = 2.5 \times 10^5$ particles.

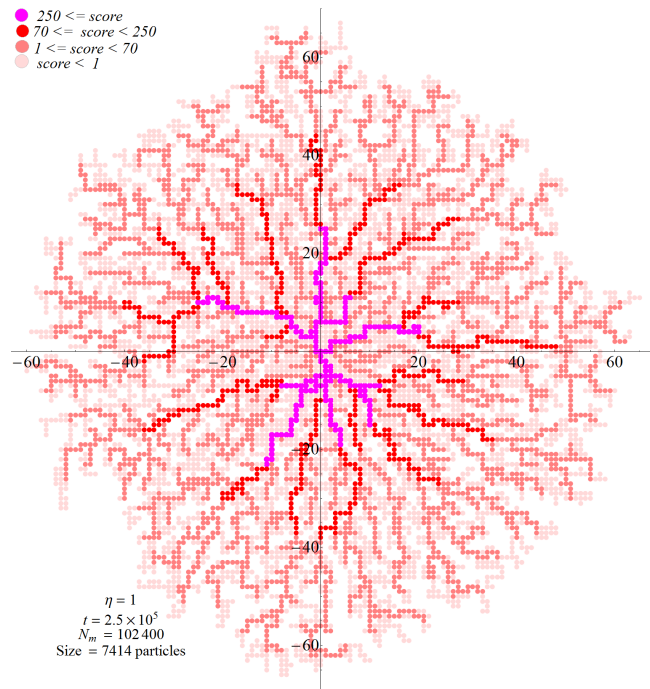


Figure 33: The same cluster as the figure (32). Different colors of the particles stand for the different values of the score associated with the corresponding particle.

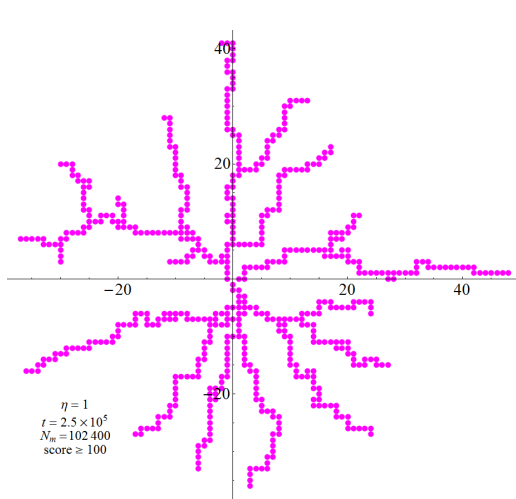


Figure 34: The same cluster as at the figure (32). Only those particles are shown which have the score ≥ 100 . The seed particle is not depicted.

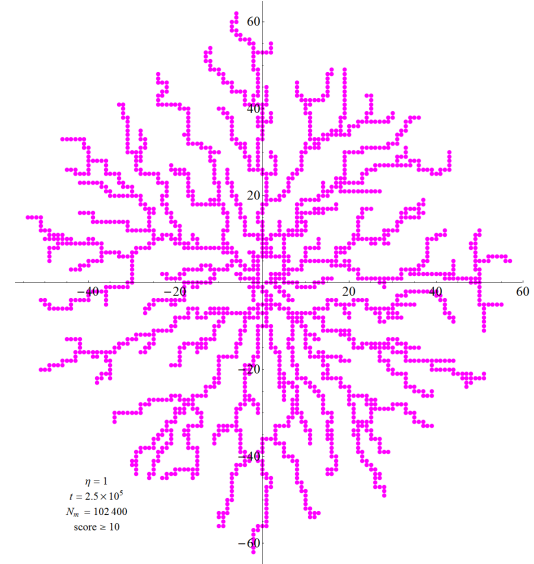


Figure 35: The same cluster as at the figure (32). Only those particles are shown which have the score ≥ 10 . The seed particle is not depicted.

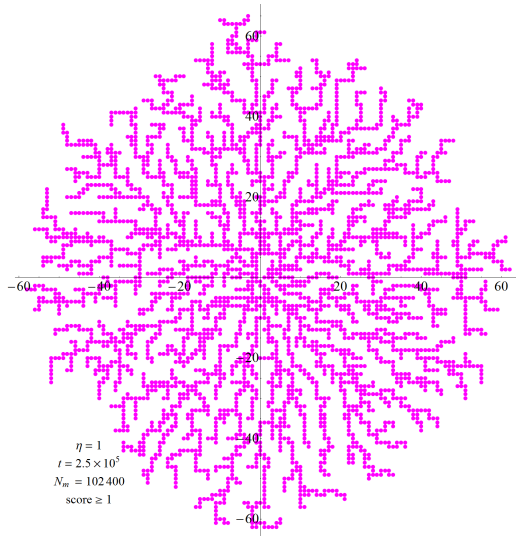


Figure 36: The same cluster as at the figure (32). Only those particles are shown which have the score ≥ 1 . The seed particle is not depicted.

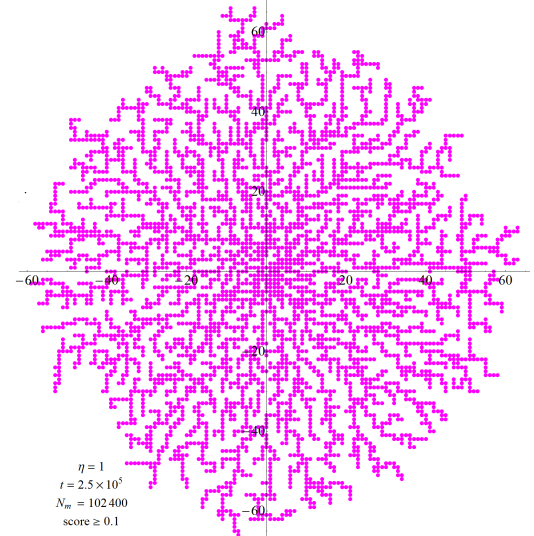


Figure 37: The same cluster as at the figure (32). Only those particles are shown which have the score ≥ 0.1 . The seed particle is not depicted.

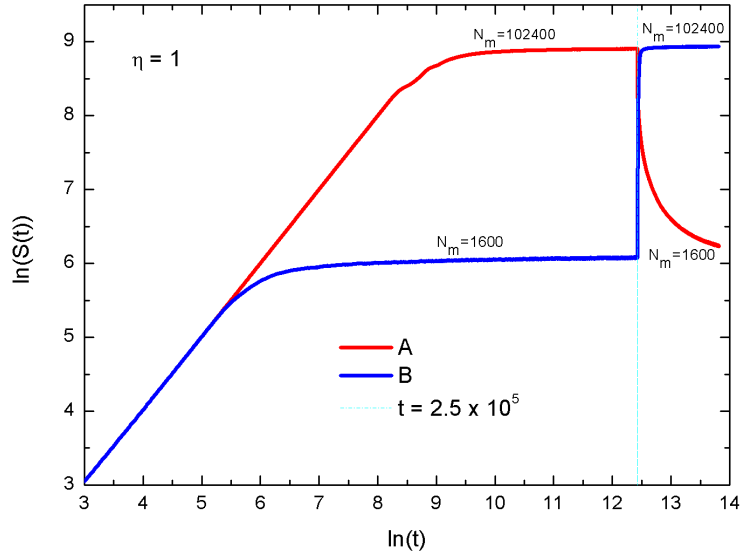


Figure 38: An illustration of the adaptive nature of the model. The evolution of the cluster size is shown for two simulations. In the first simulation (A) the value of the parameter N_m is switched from 102400 to 1600 at $t = 2.5 \times 10^5$. In the second simulation (B) N_m is switched from 1600 to 102400 at $t = 2.5 \times 10^5$. $\eta = 1$.

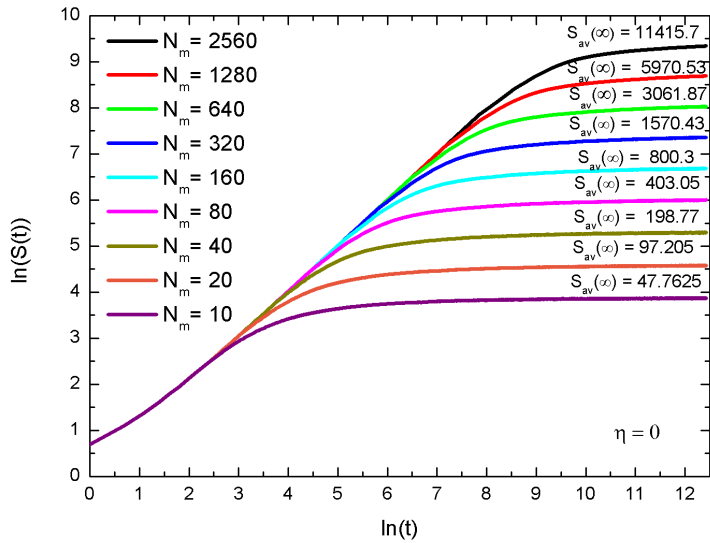


Figure 39: The evolution of the size of the cluster as the function of added particles to the cluster for different values of N_m . $\eta = 0$. The total number of the particles added to the cluster at the end of simulation is $t = 2.5 \times 10^5$.

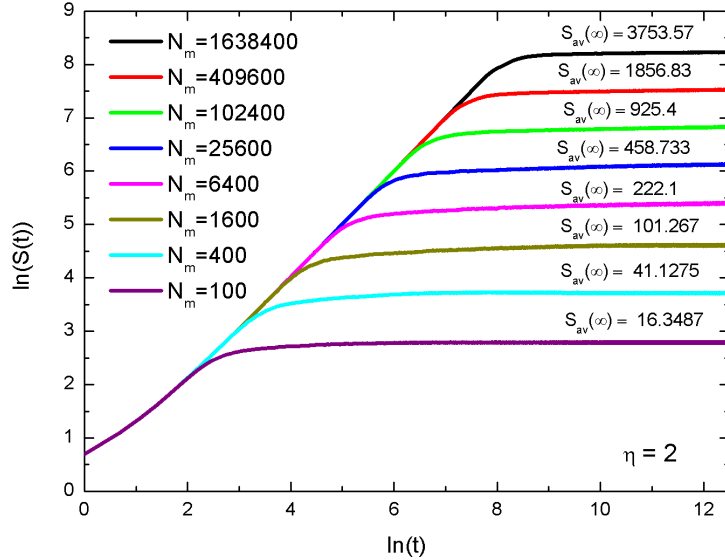


Figure 40: The evolution of the size of the cluster as the function of added particles to the cluster for different values of N_m . $\eta = 2$. The total number of the particles added to the cluster at the end of simulation is $t = 2.5 \times 10^5$.

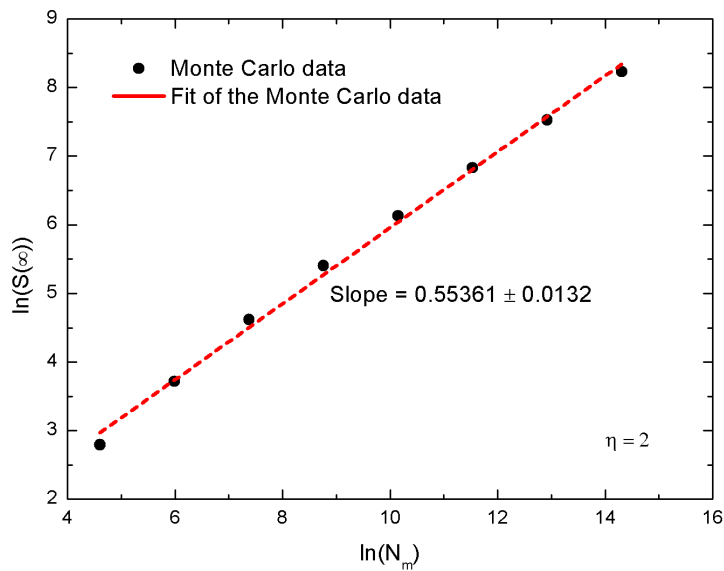


Figure 41: Dependence of the $\ln(S(\infty))$ on the $\ln(N_m)$ for clusters at the latest stage of formation reached in the current study. $\eta = 2$.

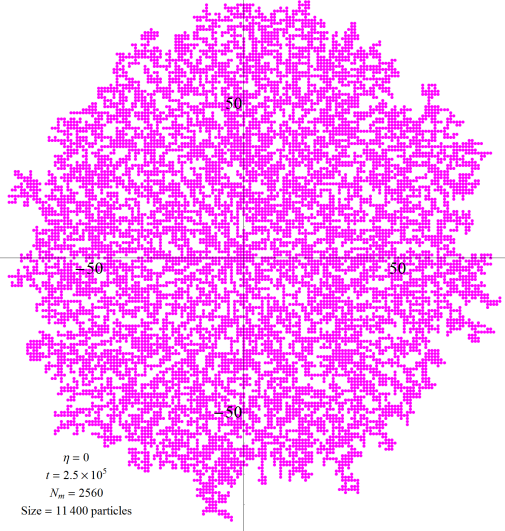


Figure 42: Typical cluster of the adaptive growth model generated with $\eta = 0$ and $N_m = 2560$ after the addition of $t = 2.5 \times 10^5$ particles.

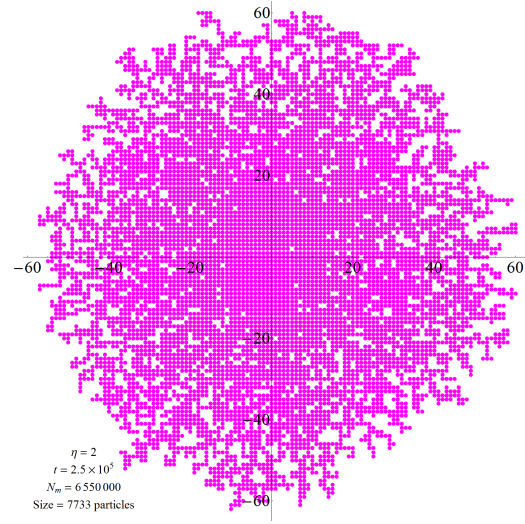


Figure 43: Typical cluster of the adaptive growth model generated with $\eta = 2$ and $N_m = 6550000$ after the addition of $t = 2.5 \times 10^5$ particles..

4 Conclusions

During the work under the current project we have gained a basic knowledge of fractal structures and possible physical systems where the fractal formation might occur. In order to underline the relevance of the problem, a brief survey of the literature on the subject is made.

By means of the Monte Carlo method we have studied the DLA model of the irreversible fractal growth and the Eden model for the adaptive network formation. For the DLA model we have investigated the two- and three-dimensional cluster growth from a seed particle fixed in the center of a system for the different values of the sticking probabilities. The effect of the sticking probability is examined over the wide range of its values at the first and second nearest neighbor sites. More over, we have also studied the DLA model for the fractal growth in the case of multiple mobile clusters.

We have examined two methods of the computing of the fractal dimension. The first method is based on the computation of the radius of gyration and the second method is due to the computation of the density-density correlations. We have shown that both methods give very close results. For the computation of the critical exponents we have created our own C++ program which is able to fit the data with a polynomial of any desired degree.

We have investigated the adaptive nature of the steady state regime of the adaptive networks formation. And pointed out the main dependencies on the model parameters.

Most of the results from the papers ([7],[10],[12]) are nicely reproduced. Some of the results are even outperformed. We have demonstrated how the averaging over several realizations of the single simulation data allows for the decrease of the random fluctuations.

One the most challenging problems from the programming point of view was the proper processing of a large data arrays for the big numbers of particles in order to reduce the computational time. And we have successfully coped with this task.

We have gone beyond the scope of the offered tasks for the project and proposed reference

literature. First of all we have used much larger statistics for the averaging compared to the ([7],[10],[12]). We have also shown that in the case of the adaptive network formation (via Eden model) strongly correlated fractal structure is obtained if the path between a newly added particle and the seed particle is defined as the shortest path. Next, in the case of the 3D DLA cluster growth we have computed the density-density correlation function and the corresponding fractal dimensions. We have shown that in this case the density-density correlation function does not depend strongly on the size of the cluster and consequently gives reasonable values for the fractal dimensions.

5 Literature

References

- [1] *Wikipedia, the free encyclopedia*, March 2011
<http://www.wikipedia.org>
- [2] B. B. Mandelbrot: *The Fractal Geometry of Nature*,
W .H. Freedman and Company, ISBN 0-1767-1186-9, 1983
- [3] K. Falconer: *Fractal Geometry, Mathematical Foundations and Application*,
John Wiley & Sons, ISBN 0 471 92287 0, 1990
- [4] T. Vicsek: *Fractal Growth Phenomena*, Second Edition
World Scientific Publishing Co. Pte. Ltd., ISBN 9810206690, 1999
- [5] S. F. Edwards, M. Schwartz: *Exact differential equations for diffusion limited aggregation*,
Physica A 227, 1996
- [6] T. A. Witten, L. M. Sander: *Diffusion-Limited Aggregation, a Kinetic Critical Phenomenon*, Phys.Rev.Lett. 47, N 19, 1981
- [7] P. Meakin: *Diffusion-controlled cluster formation in 2–6-dimensional space*,
Phys.Rev. A 27, N 3, 1983
- [8] P. Meakin: *Progress in DLA research*, Physica D 86, 1995
- [9] P. Meakin: *Fractals, scaling and growth far from equilibrium*,
Cambridge University Press, ISBN 0 521 45253 8, 1998
- [10] P. Meakin: *Formation of Fractal Clusters and Networks by Irreversible Diffusion-Limited Aggregation*, Phys.Rev.Lett. 51, N 13, 1983
- [11] M. Eden: *A Two-Dimensional Growth Process*,
University of California Press, Proc. Fourth Berkeley Symp. on Math. Statist. and Prob., Vol 4, 1961
- [12] P. Meakin: *An Eden model for the growth of adaptive networks*,
Physica A 179, 1991
- [13] J. M. Costa, F. Sagués, M. Vilarrasa: *Growth rate of fractal copper electrodeposits: Potential and concentration effects*, Phys.Rev. A 43, N 12, 1991
- [14] R. Seshadri, G. N. Subbanna, V. Vijayakrishnan, G. U. Kulkarni, G. Ananthakrishna, C. N. R. Rao: *Growth of Nanometric Gold Particles in Solution Phase*, J.Phys.Chem. 99, 1995

A Additional data from 2D DLA clusters simulation ($p_{nn} = 1$)

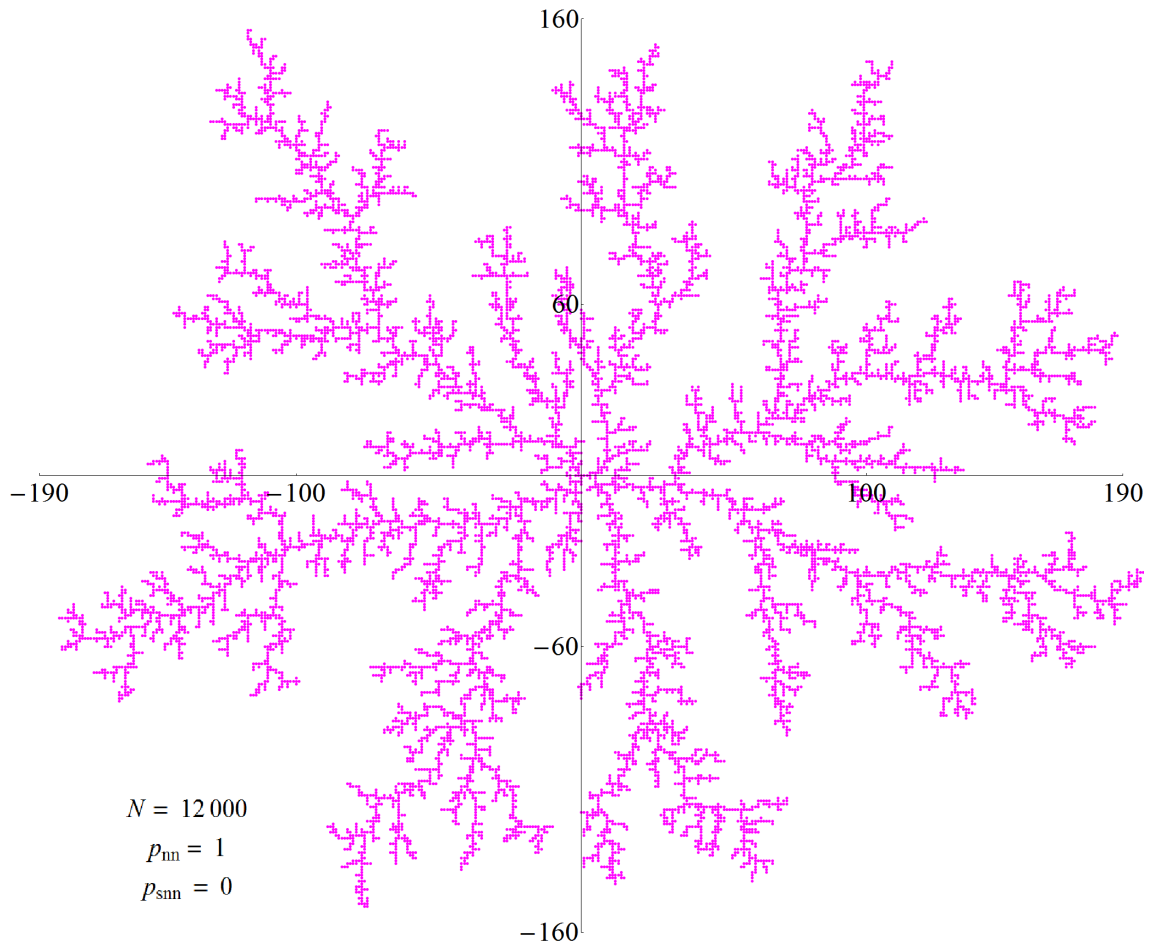


Figure 44: Typical two dimensional cluster of $N = 12000$ particles obtained from the Monte Carlo simulation of DLA growth from the seed particle fixed in the center of the system. Sticking probability at the nearest neighbor sites p_{nn} is 1.

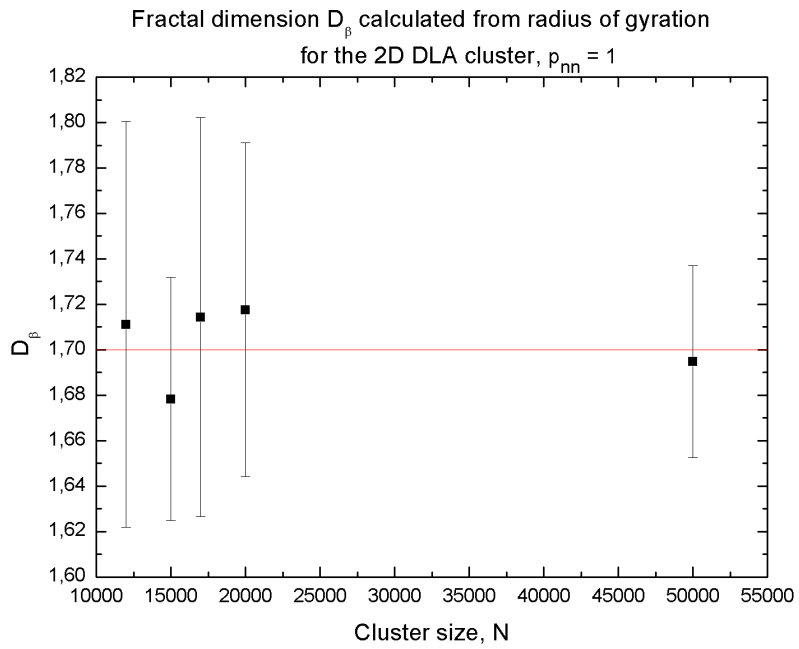


Figure 45: Computed via linear fit of $\ln(R_g(N))$ over the last 95% of particles added to the clusters

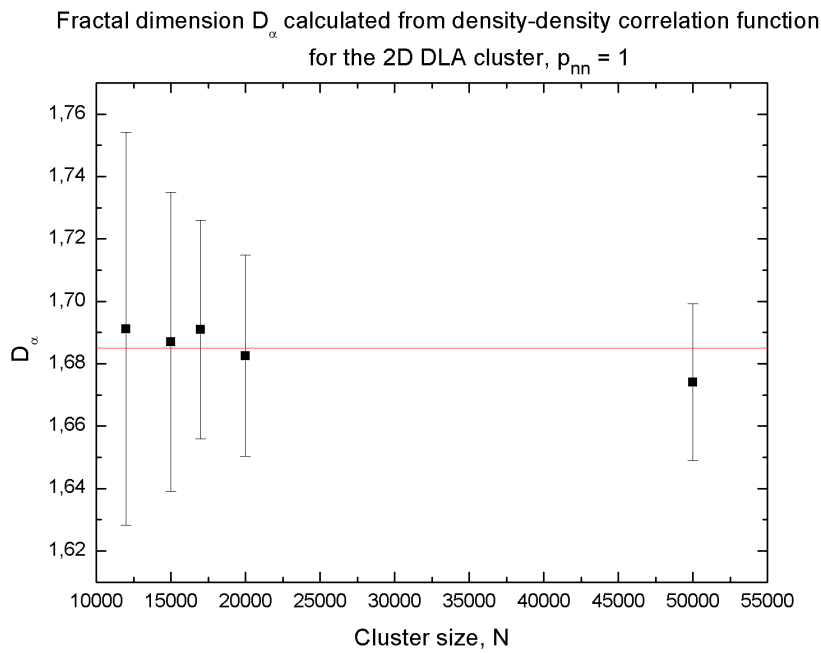


Figure 46

B Additional data from 2D DLA clusters simulation ($p_{nn} < 1$, $p_{snn} = 0$)

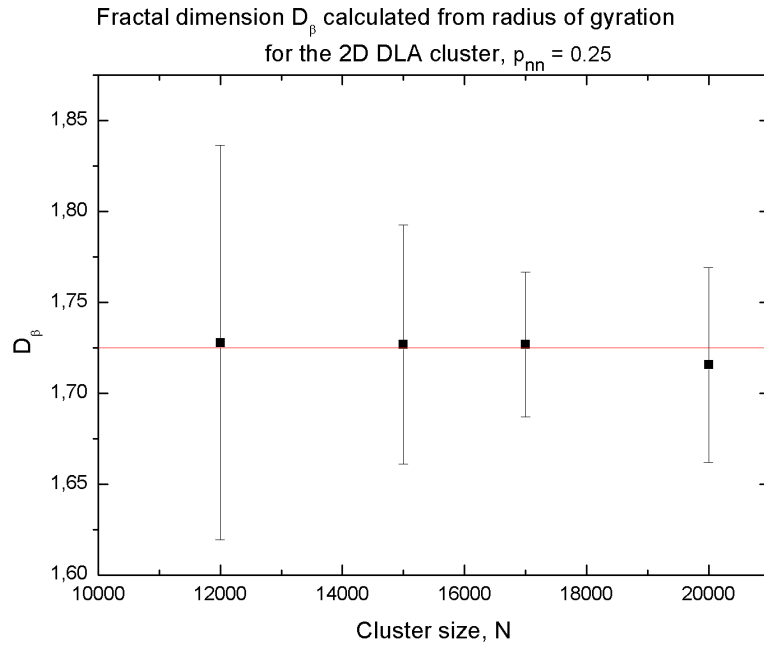


Figure 47: Computed via linear fit of $\ln(R_g(N))$ over the last 95% of particles added to the clusters

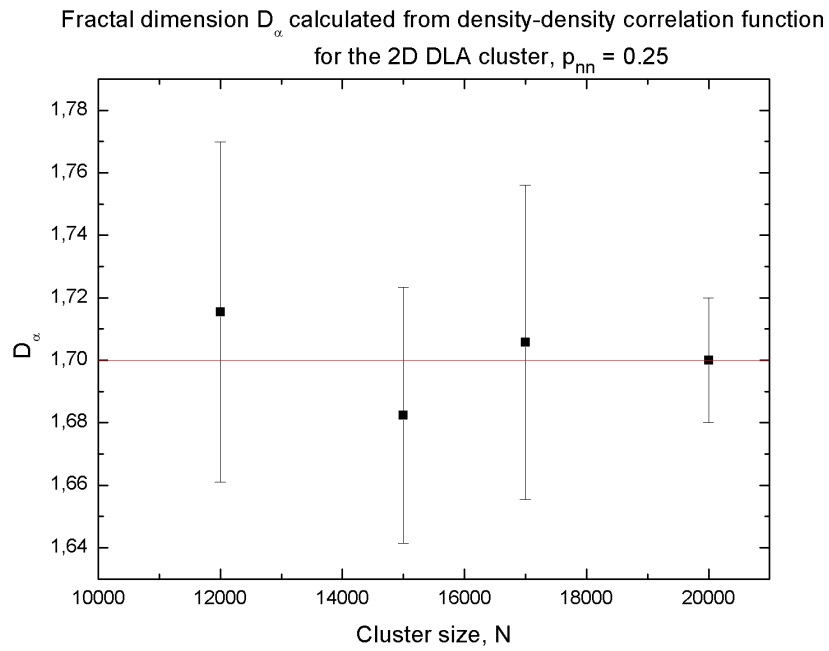


Figure 48

p_{nn}	N	Radius of gyration exponent, β				Density-density correlation function exponent, α	Coordination number
		50%	75%	90%	95%		
0.1	12000	0.5811 \pm 0.0404	0.5746 \pm 0.0287	0.5694 \pm 0.0236	0.5657 \pm 0.0201	0.2761 \pm 0.0528	2.8144 \pm 0.0142
0.1	20000	0.5867 \pm 0.0371	0.582 \pm 0.041	0.5755 \pm 0.0309	0.5714 \pm 0.0298	0.2886 \pm 0.0454	2.8138 \pm 0.0122
0.25	12000	0.577 \pm 0.0297	0.5784 \pm 0.0378	0.58 \pm 0.038	0.5787 \pm 0.0364	0.2845 \pm 0.0544	2.586 \pm 0.0163
0.25	15000	0.5832 \pm 0.0132	0.58 \pm 0.019	0.58 \pm 0.023	0.579 \pm 0.022	0.3176 \pm 0.0409	2.592 \pm 0.012
0.25	17000	0.5763 \pm 0.0133	0.5801 \pm 0.0146	0.5801 \pm 0.0126	0.5791 \pm 0.0134	0.2943 \pm 0.0503	2.59 \pm 0.01
0.25	20000	0.5804 \pm 0.0351	0.5803 \pm 0.0299	0.5822 \pm 0.0191	0.5829 \pm 0.0182	0.3 \pm 0.02	2.5903 \pm 0.0083
0.4	12000	0.5824 \pm 0.023	0.585 \pm 0.0245	0.5798 \pm 0.0284	0.5774 \pm 0.0254	0.3185 \pm 0.0782	2.4606 \pm 0.0173
0.4	20000	0.5837 \pm 0.0257	0.5862 \pm 0.0339	0.5865 \pm 0.0271	0.5851 \pm 0.0219	0.3081 \pm 0.0285	2.4641 \pm 0.0086
0.7	12000	0.583 \pm 0.021	0.5815 \pm 0.0289	0.5806 \pm 0.0288	0.5808 \pm 0.0278	0.3031 \pm 0.0486	2.2967 \pm 0.0122

Table 5: Results obtained from the simulation of DLA cluster formation on two dimensional simple cubic lattice with a sticking probability at the nearest neighbor sites $p_{nn} < 1$ and at the second nearest neighbor sites $p_{snn} = 0$. All values of α , β and coordination number are averaged over 10 clusters.

p_{nn}	N	D_β				D_α
		50%	75%	90%	95%	
0.1	12000	1.7209 \pm 0.1196	1.74 \pm 0.087	1.7562 \pm 0.0726	1.7678 \pm 0.0629	1.7239 \pm 0.0528
0.1	20000	1.7044 \pm 0.1077	1.719 \pm 0.121	1.7376 \pm 0.0932	1.7501 \pm 0.0913	1.7116 \pm 0.0454
0.25	12000	1.7333 \pm 0.0891	1.729 \pm 0.113	1.7244 \pm 0.1129	1.7279 \pm 0.1085	1.7155 \pm 0.0544
0.25	15000	1.7147 \pm 0.0396	1.724 \pm 0.055	1.7242 \pm 0.0738	1.7269 \pm 0.0657	1.6824 \pm 0.0409
0.25	17000	1.74 \pm 0.04	1.7239 \pm 0.0433	1.7238 \pm 0.0373	1.7268 \pm 0.0398	1.7057 \pm 0.0503
0.25	20000	1.723 \pm 0.104	1.7234 \pm 0.0889	1.7175 \pm 0.0563	1.7156 \pm 0.0535	1.7 \pm 0.02
0.4	12000	1.7169 \pm 0.0679	1.7095 \pm 0.0717	1.7247 \pm 0.0845	1.732 \pm 0.076	1.6815 \pm 0.0782
0.4	20000	1.7131 \pm 0.0755	1.7059 \pm 0.0987	1.7051 \pm 0.0787	1.709 \pm 0.064	1.6919 \pm 0.0285
0.7	12000	1.715 \pm 0.061	1.7196 \pm 0.0854	1.7224 \pm 0.0855	1.7219 \pm 0.0824	1.6969 \pm 0.0486

Table 6: Fractal dimension computed from the radius of gyration and density-density correlation function given in table (5).

C Additional data from 2D DLA clusters simulation ($p_{nn} = 0$, $p_{snn} \neq 0$)

p_{snn}	N	Radius of gyration exponent, β				Density-density correlation function exponent, α
		50%	75%	90%	95%	
1	12000	0.579±0.031	0.58±0.025	0.5817±0.0226	0.5818±0.0211	0.3021±0.0235
1	15000	0.5923±0.0458	0.5918±0.0264	0.59±0.03	0.5889±0.0274	0.3174±0.0449
1	17000	0.58±0.03	0.5863±0.0227	0.5896±0.0269	0.5906±0.0232	0.317±0.023
1	20000	0.5887±0.0243	0.5877±0.0238	0.5847±0.0193	0.5821±0.0185	0.3257±0.0346
0.7	12000	0.5936±0.0241	0.595±0.025	0.5949±0.0218	0.5921±0.0205	0.319±0.026
0.25	12000	0.5832±0.0355	0.5895±0.0174	0.5864±0.0195	0.5832±0.0218	0.3197±0.0472
0.1	12000	0.5839±0.0257	0.5855±0.0159	0.584±0.018	0.5817±0.0239	0.3025±0.0497
0.1	15000	0.5837±0.0327	0.578±0.043	0.573±0.041	0.5714±0.0383	0.2905±0.0494
0.1	17000	0.5881±0.0291	0.5862±0.0297	0.5783±0.0253	0.5751±0.0203	0.2896±0.0292
0.1	20000	0.5773±0.0472	0.5774±0.0319	0.5774±0.0243	0.58±0.02	0.2919±0.0305

Table 7: Results obtained from the simulation of DLA cluster formation on two dimensional simple cubic lattice with a sticking probability at the nearest neighbor sites $p_{nn} = 0$ and at the second nearest neighbor sites $p_{snn} \neq 0$. All values of α , β and coordination number are averaged over 10 clusters.

p_{snn}	N	D_β				D_α
		50%	75%	90%	95%	
1	12000	1.727±0.091	1.7248±0.0742	1.7191±0.0668	1.7189±0.0623	1.6979±0.0235
1	15000	1.6883±0.1305	1.6897±0.0753	1.6979±0.0868	1.698±0.079	1.6826±0.0449
1	17000	1.7107±0.0877	1.7057±0.0661	1.696±0.0773	1.6936±0.0664	1.683±0.025
1	20000	1.7±0.07	1.7016±0.0688	1.7104±0.0565	1.7178±0.0545	1.6743±0.0346
0.7	12000	1.6847±0.0685	1.68±0.07	1.681±0.062	1.689±0.059	1.681±0.026
0.25	12000	1.7146±0.1043	1.7±0.05	1.7053±0.0567	1.7147±0.0642	1.6803±0.0472
0.1	12000	1.7126±0.0753	1.7078±0.0463	1.7124±0.0522	1.7192±0.0708	1.6975±0.0497
0.1	15000	1.713±0.096	1.7315±0.1288	1.7463±0.1252	1.7501±0.1172	1.7095±0.0494
0.1	17000	1.7004±0.0843	1.7058±0.0866	1.7292±0.0755	1.73886±0.0612	1.7105±0.0292
0.1	20000	1.7322±0.1416	1.7318±0.0957	1.7319±0.0728	1.7301±0.0605	1.7081±0.0305

Table 8: Fractal dimension computed from the radius of gyration and density-density correlation function given in table (7).

D Additional data from 2D DLA clusters simulation ($p_{nn} \neq 0, p_{snn} \neq 0$)

p_{nn}	p_{snn}	N	Radius of gyration exponent, β				Density-density correlation function exponent, α	Coordination number
			50%	75%	90%	95%		
0.1	0.1	12000	0.5885±0.0341	0.5835±0.0354	0.5806±0.0276	0.5797±0.0316	0.3034±0.0415	1.6446±0.0257
0.1	1	12000	0.5906±0.0367	0.5918±0.0362	0.5935±0.0423	0.59±0.04	0.3237±0.0355	0.0809±0.0058
1	0.1	12000	0.5737±0.0349	0.5707±0.0281	0.5722±0.0207	0.5725±0.0176	0.2964±0.0443	1.9856±0.0065
1	1	12000	0.591±0.023	0.5892±0.0228	0.59±0.02	0.5898±0.0122	0.3257±0.0339	0.5902±0.0139
0.7	0.7	12000	0.5747±0.0312	0.5732±0.0333	0.5704±0.0282	0.5695±0.0262	0.3112±0.0299	0.832±0.015
0.1	0.1	15000	0.5734±0.0424	0.5787±0.0393	0.583±0.026	0.5837±0.0195	0.3198±0.0462	1.6469±0.0213
0.1	1	15000	0.5827±0.0261	0.5828±0.0206	0.5812±0.0237	0.58±0.03	0.32±0.04	0.0787±0.0041
1	0.1	15000	0.5823±0.0245	0.5827±0.0259	0.581±0.017	0.5826±0.0193	0.3119±0.0439	1.9825±0.0108
1	1	15000	0.6005±0.0438	0.5949±0.0492	0.5913±0.0425	0.5895±0.0357	0.326±0.028	0.5854±0.0183
0.7	0.7	15000	0.5808±0.0266	0.5812±0.0226	0.5856±0.029	0.587±0.0277	0.3246±0.0169	0.8164±0.0119

Table 9: Results obtained from the simulation of DLA cluster formation on two dimensional simple cubic lattice with a sticking probability at the nearest neighbor sites $p_{nn} \neq 0$ and at the second nearest neighbor sites $p_{snn} \neq 0$. All values of α , β and coordination number are averaged over 10 clusters.

p_{nn}	p_{snn}	N	D_β				D_α
			50%	75%	90%	95%	
0.1	0.1	12000	1.6993±0.0984	1.714±0.104	1.7224±0.0819	1.725±0.094	1.6966±0.0415
0.1	1	12000	1.6933±0.1053	1.6899±0.1035	1.69±0.12	1.6891±0.1131	1.6764±0.0355
1	0.1	12000	1.743±0.106	1.7521±0.0863	1.7476±0.0631	1.7468±0.0536	1.7036±0.0443
1	1	12000	1.6912±0.0658	1.6973±0.0656	1.695±0.049	1.6957±0.0352	1.6743±0.0339
0.7	0.7	12000	1.74±0.09	1.7447±0.1014	1.7531±0.0867	1.7558±0.0807	1.6889±0.0299
0.1	0.1	15000	1.7439±0.1289	1.728±0.117	1.715±0.075	1.7132±0.0572	1.6802±0.0462
0.1	1	15000	1.7162±0.0769	1.7158±0.0606	1.7206±0.0702	1.7242±0.0954	1.68±0.04
1	0.1	15000	1.7175±0.0723	1.7162±0.0764	1.7213±0.0518	1.7164±0.0569	1.6881±0.0439
1	1	15000	1.6654±0.1213	1.6811±0.1391	1.6912±0.1216	1.6963±0.1027	1.6741±0.0278
0.7	0.7	15000	1.722±0.079	1.7205±0.0669	1.7076±0.0845	1.7032±0.0802	1.6754±0.0169

Table 10: Fractal dimension computed from the radius of gyration and density-density correlation function given in table (9).

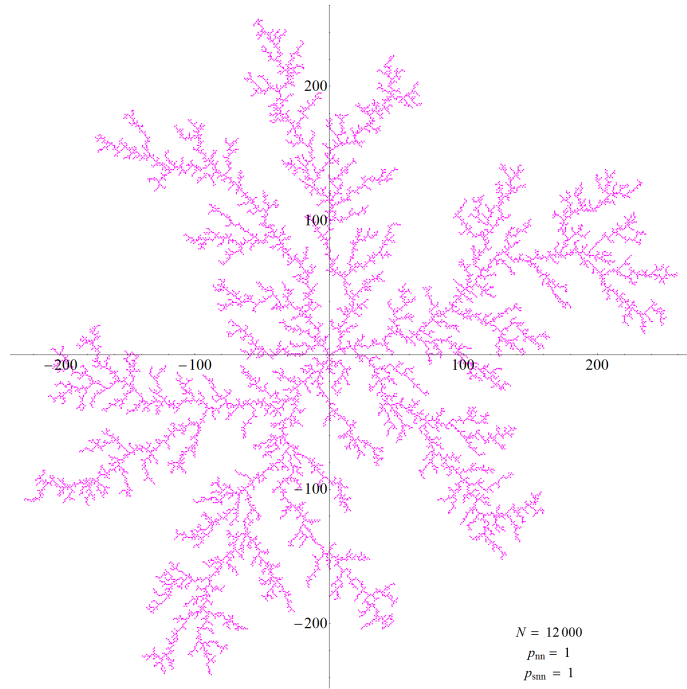


Figure 49: Typical two dimensional cluster of $N = 12000$ particles obtained from the Monte Carlo simulation of DLA growth from the seed particle fixed in the center of the system. $p_{nn} = 1$ and $p_{snn} = 1$.

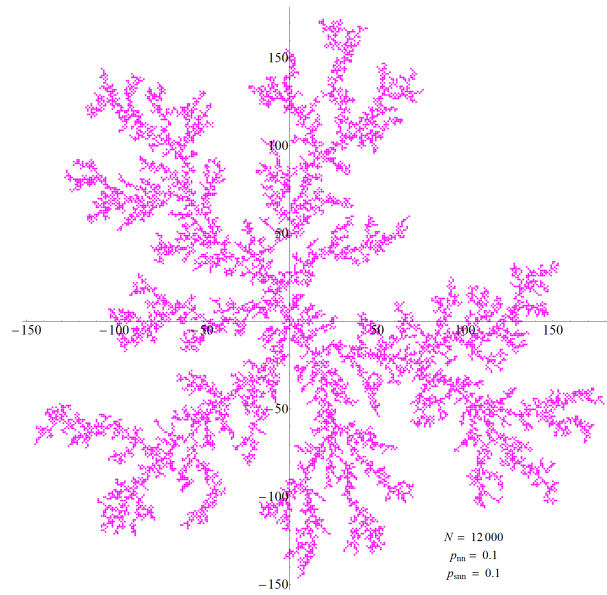


Figure 50: Typical two dimensional cluster of $N = 12000$ particles obtained from the Monte Carlo simulation of DLA growth from the seed particle fixed in the center of the system. $p_{nn} = 0.1$ and $p_{snn} = 0.1$.

E Additional data from 3D DLA clusters simulation ($p_{nn} = 1$ and $p_{nn} = 0.25$)

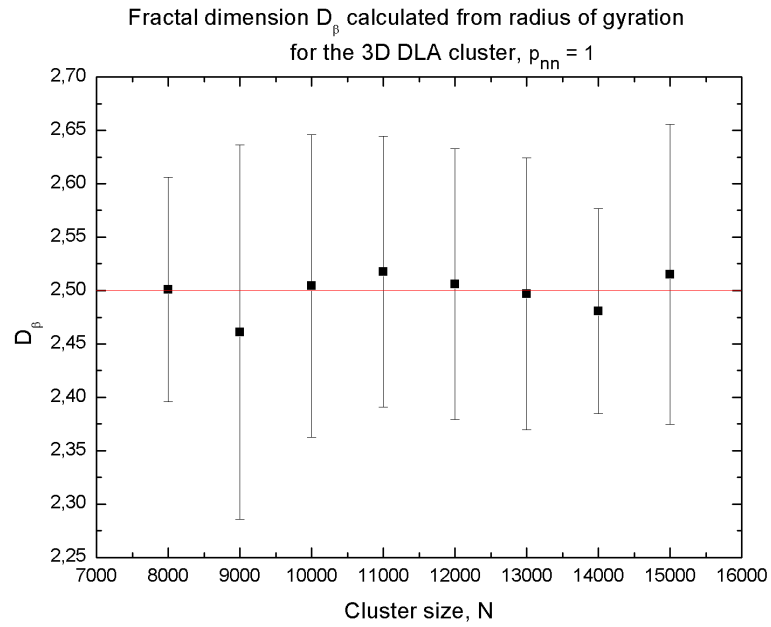


Figure 51: Computed via linear fit of $\ln(R_g(N))$ over the last 95% of particles added to the clusters

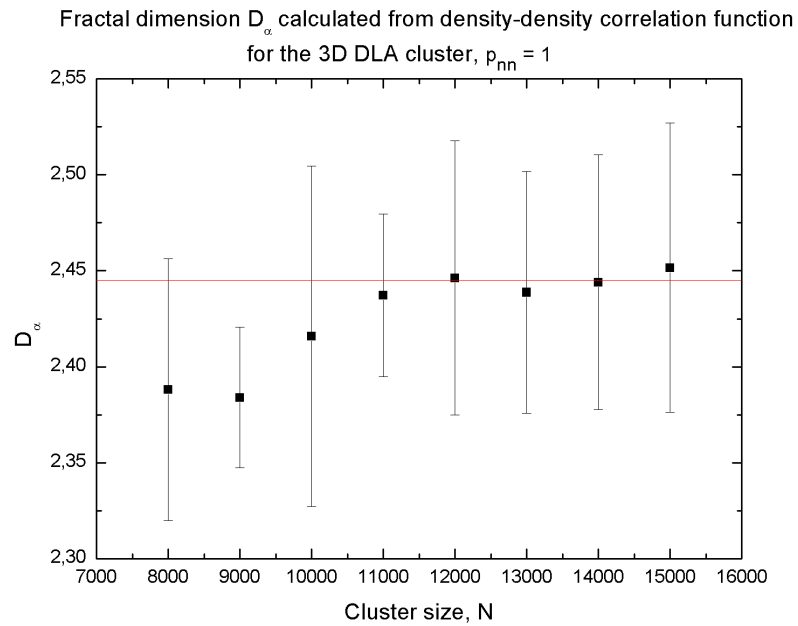


Figure 52

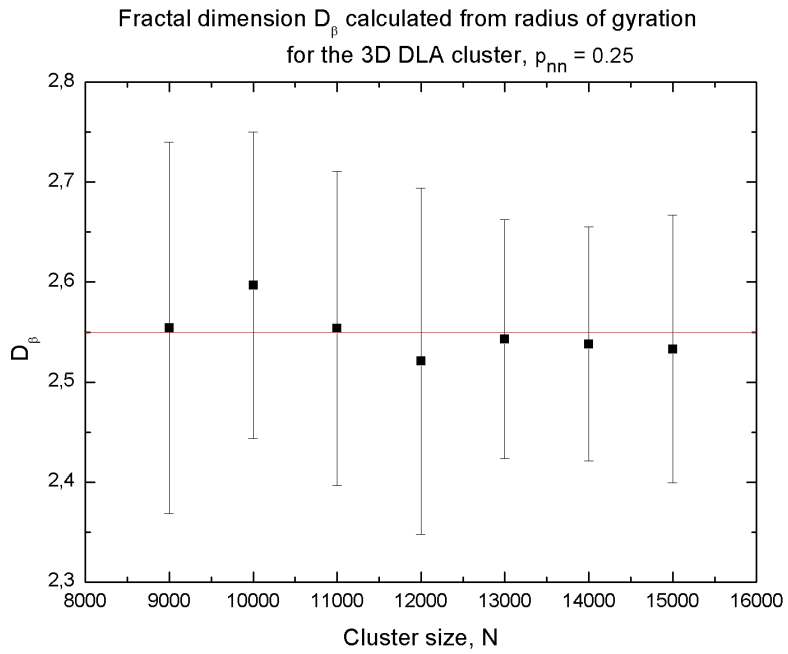


Figure 53: Computed via linear fit of $\ln(R_g(N))$ over the last 95% of particles added to the clusters

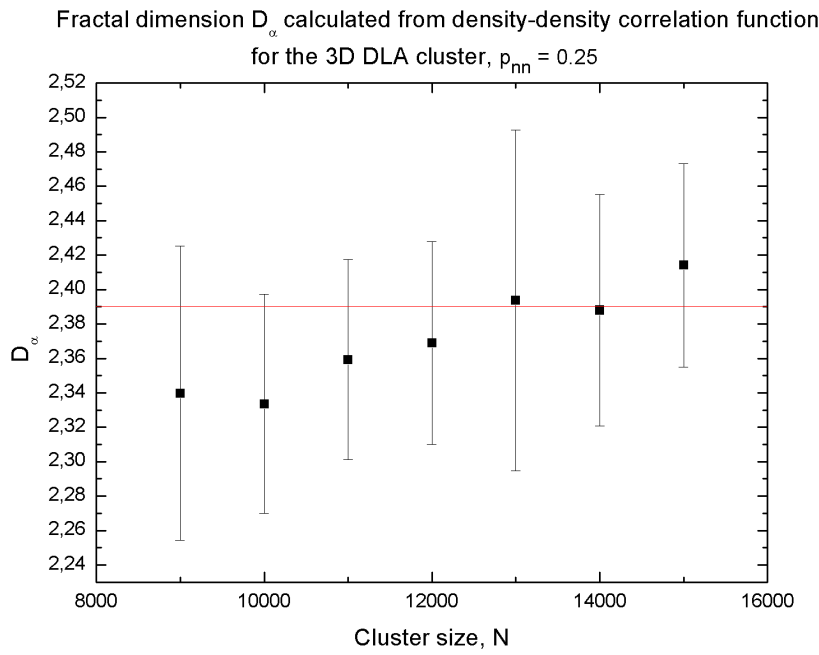


Figure 54

N	Radius of gyration exponent, β				α
	50%	75%	90%	95%	
9000	0.39029±0.04002	0.39374±0.03620	0.39335± 0.03034	0.39151±0.02848	0.66028±0.08556
10000	0.39426±0.02018	0.39092±0.01921	0.38710± 0.01935	0.38511±0.02273	0.66641±0.06377
11000	0.38994±0.01460	0.38961±0.01775	0.39084± 0.02221	0.39161±0.02410	0.64082±0.05811
12000	0.39667±0.02806	0.39644±0.03612	0.39723± 0.03090	0.39669±0.02724	0.63110±0.05904
13000	0.39163±0.02191	0.39208±0.02593	0.39244± 0.02250	0.39327±0.01849	0.60633±0.09909
14000	0.39538±0.02546	0.39750±0.01449	0.39578± 0.01539	0.39403±0.01817	0.61198±0.06724
15000	0.39451±0.02624	0.39541±0.02688	0.39570± 0.02054	0.39478±0.02089	0.58598±0.05896
N	D_β				D_α
9000	2.56222±0.26276	2.53973±0.23347	2.54227± 0.19609	2.55422±0.18580	2.33972±0.08556
10000	2.53638±0.12982	2.55804±0.12573	2.58333± 0.12913	2.59664±0.15326	2.33359±0.06377
11000	2.56450±0.09602	2.56666±0.11697	2.55859± 0.14536	2.55354±0.15711	2.35918±0.05811
12000	2.52097±0.17833	2.52243±0.22979	2.51742± 0.19583	2.52089±0.17314	2.36890±0.05904
13000	2.55343±0.14285	2.55048±0.16867	2.54815± 0.14613	2.54276±0.11955	2.39367±0.09909
14000	2.52920±0.16286	2.51572±0.09171	2.52665± 0.09825	2.53789±0.11703	2.38802±0.06724
15000	2.53480±0.16860	2.52901±0.17195	2.52714± 0.13118	2.53303±0.13407	2.41402±0.05896
N	Projected area exponent, γ				
9000	0.81899±0.06121	0.82145±0.06883	0.81605± 0.05254	0.81731±0.04727	
10000	0.81726±0.07444	0.82205±0.08222	0.82276± 0.06070	0.82281±0.05409	
11000	0.82666±0.06412	0.82850±0.05630	0.82372± 0.05283	0.81864±0.04654	
12000	0.83658±0.05679	0.83160±0.04495	0.82980± 0.03346	0.83187±0.02418	
13000	0.83007±0.06207	0.83368±0.03860	0.83009± 0.03560	0.83075±0.02661	
14000	0.82711±0.07154	0.83435±0.05726	0.83276± 0.04602	0.83062±0.04066	
15000	0.82245±0.02484	0.81742±0.02703	0.82045± 0.02901	0.82108±0.02702	

Table 11: Results obtained from the simulation of DLA cluster formation on the three dimensional simple cubic lattice. $p_{nn} = 0.25$. All values of α , β , D_α , D_β and γ are averaged over 10 clusters.

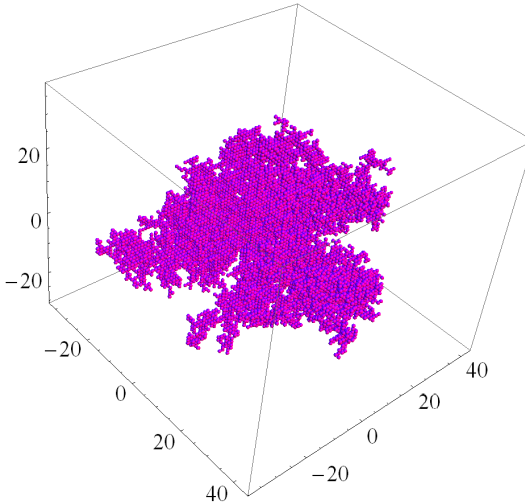


Figure 55: Typical three dimensional cluster of $N = 14000$ particles obtained from the Monte Carlo simulation of DLA growth from the seed particle fixed in the center of the system. $p_{nn} = 0.25$ and $p_{sn} = 0$.

F Additional data from adaptive network simulation

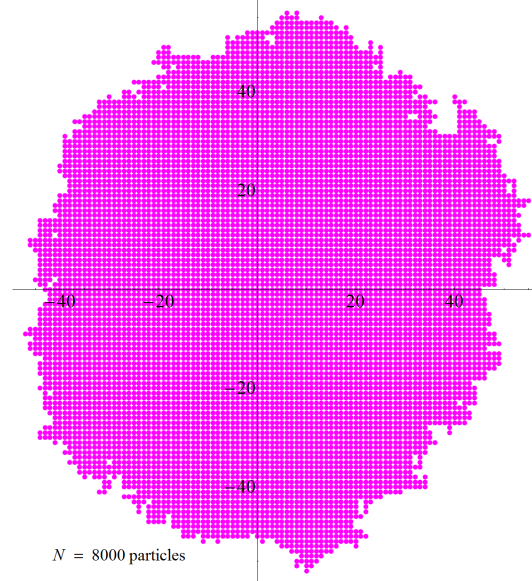


Figure 56: Typical Eden cluster of $N = 8000$ particles. In the original Eden model [11] particles are not deleted from the cluster. New particles are added on the perimeter of the cluster with the probability proportional to the number of the nearest neighbor sites already occupied by the particles from the cluster.

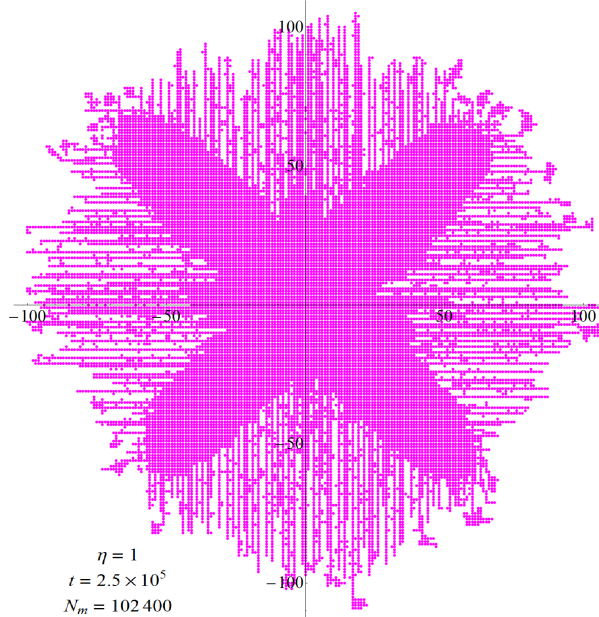


Figure 57: Adaptive network cluster formed after 2.5×10^5 particles were added to the cluster. This figure demonstrates that the condition for the score to be increased only for particles in the shortest path between newly added particle and the seed particle in the center imposes substantial non-random correlations on the entire structure of the cluster.